Latency-Aware Metaverse Rendering in Vehicular Edge Networks: A Secrecy-Oriented Resource Allocation Approach

Xin Li, Minghui Dai, *Member, IEEE*, Shan Chang, *Member, IEEE*, Liang Zhang, Tianshun Wang, *Member, IEEE*, Jiaming Pei, *Member, IEEE*, and Shahid Mumtaz, *Senior Member, IEEE*

***Abstract*—The development of vehicular networks and artificial intelligence (AI) technologies has driven the application of Metaverse in vehicular field. However, the limited resources of vehicular networks pose significant challenges to the real-time rendering of vehicular Metaverse, with the core bottleneck being high computational and transmission delays. In addition, the secrecy communication in vehicular networks is critical to Metaverse rendering. In this paper, we propose a latency-aware Metaverse rendering scheme in vehicular edge networks aimed at enhancing the users' quality of experience (QoE). We design a collaborative rendering architecture, where the background elements and foreground objects are rendered in different layers by the Metaverse provider server (MPS), the roadside unit (RSU), and local terminals. Meanwhile, in the transmission link, we have taken secure communication into consideration. A joint optimization problem is constructed to minimize the total rendering delay of the system, synchronously optimizing the offloading strategy, confidentiality interruption strategy, and transmission latency strategy. To address the non-convexity of the problem, a hierarchical solution method is proposed, which converts it into convex subproblems to obtain the optimal solutions. Simulations show that the proposed scheme outperforms traditional schemes in terms of performance and computational efficiency.**

***Index Terms*—Metaverse rendering, quality of experience, vehicular networks.**

I. Introduction

In RECENT years, with the advancement of vehicular networks [1], virtual reality (VR) has experienced vigorous development [2], [3], injecting fresh impetus into various fields. Riding on the wave of artificial intelligence progress, the vehicular Metaverse is poised to embrace new growth and opportunities. In future internet of vehicles scenarios, as autonomous driving technology becomes increasingly sophisticated and relevant regulations are gradually refined, vehicular users are able to deeply immerse themselves in the virtual world built by the Metaverse. This highly futuristic experience will eventually evolve from a concept into reality, providing boundless vitality for creating an entirely new digital world [4], [5]. However, traditional vehicular Metaverse rendering relies solely on VR devices with limited computational capability. This not only results in excessively long rendering delays due to insufficient computing power, which impairs the immersive experience of vehicular users, but also leads to high energy consumption and shortened service life of the devices due to heavy computing loads.

Mobile edge computing (MEC) technology provides an effective technical solution to address these core issues [6], [7], [8], [9], [10], [11]. By deploying the necessary computing and storage resources at the network edge, keeping them within close range of users, it overcomes the limitations of traditional rendering. The in-depth integration of MEC and vehicular Metaverse rendering enables rational allocation of users' immersive requests based on factors such as real-time computing power of edge nodes and complexity of rendering tasks, thus providing vehicular users with services featuring low latency, high efficiency, and scalability. However, with the rapid development of mobile internet, the demand for access technologies in communication systems is constantly growing. How to efficiently support large-scale vehicular users' connection and data transmission with limited spectrum resources, and ultimately provide users with optimal quality of experience (QoE), has become another core challenge for the future vehicular Metaverse networks.

Multi-access technology, as the core technology enabling multiple users to share the same communication resources, delivers its core value through efficient resource reuse and allocation [12], [13], [14]. It supports concurrent communication among multiple users under limited resources while reducing interference and ensuring communication quality. Requested resources from vehicular users can be transmitted via multi-access methods, simultaneously meeting the core requirements of multi-user concurrent communication, low latency, and low

Received 7 September 2025; revised 24 November 2025; accepted 20 December 2025. This work was supported in part by the National Natural Science Foundation of China under Grant 62472083 and Grant 62501137, in part by the AI-Enhanced Research Program of Shanghai Municipal Education Commission under Grant SMEC-AI-DHUZ-01, and in part by the State Key Laboratory for Novel Software Technology at Nanjing University under Grant KFKT2025B69. The review of this article was coordinated by Prof. Geng Sun. *(Corresponding author: Shan Chang.)*

Xin Li, Minghui Dai, Shan Chang, and Liang Zhang are with the School of Computer Science and Technology, Donghua University, Shanghai 201620, China (e-mail: lixin@mail.dhu.edu.cn; minghuidai@dhu.edu.cn; changshan@dhu.edu.cn; zhangliang@dhu.edu.cn).

Tianshun Wang is with the School of Communication and Information Engineering, Nanjing University of Posts and Telecommunications, Nanjing 210023, China (e-mail: tswang@njupt.edu.cn).

Jiaming Pei is with the School of Computer Science, University of Sydney, Sydney, NSW 2006, Australia (e-mail: jpei0906@uni.sydney.edu.au).

Shahid Mumtaz is with the Department of Computer Science, Nottingham Trent University, NG1 4FQ Nottingham, U.K. (e-mail: shahid.mumtaz@ntu.ac.uk).

Digital Object Identifier 10.1109/TVT.2025.3647959

energy consumption within limited communication resources [15]. This not only resolves the communication bottlenecks inherent in vehicular environments but also lays a fundamental transmission infrastructure to underpin the large-scale deployment of autonomous driving systems and vehicular Metaverse applications in the future.

In addition, security is essential for ensuring the normal operation of vehicular Metaverse systems [16], [17], [18], [19]. In vehicular edge networks, eavesdropping during wireless transmission may induce scene data leakage, rendering parameter tampering, and exposure of sensitive information (e.g., user identities, behavioral trajectories), directly compromising the security and reliability of vehicular metaverse services. Therefore, designing a resource allocation mechanism that balances confidentiality and latency optimisation has become a critical prerequisite for ensuring the reliable implementation of Metaverse services in vehicular edge networks.

To ensure the quality of users' immersive experience, the trade-off between Metaverse experience metrics and terminal energy consumption has been investigated in [20], which addresses the Metaverse resource allocation. However, this solution is highly dependent on attention data and has limited scalability in complex scenarios. A collaborative VR rendering and dynamic resource leasing mechanism has been studied in [2], aiming to address the rendering latency and visual quality simultaneously. Nevertheless, this scheme incurs high training costs, and fails to take security performance into account. In addition, due to the priority given to users' QoE, there is still room for improvement in terms of resource utilization efficiency. Meanwhile, a collaborative rendering framework and a multi-object real-time rendering workflow have been exploited in [3]. It minimizes the motion-to-photon latency by jointly optimizing the rendering positions of foreground objects and bandwidth resources. However, this scheme fails to take into account complex and variable channel conditions as well as security performance, which leads to certain impacts on channel transmission rate and stability.

Aiming to tackle the aforementioned challenges, we propose a secrecy-oriented resource allocation method for latency-aware Metaverse rendering in vehicular edge networks. It aims to minimize the total rendering delay while ensuring the secure transmission of rendering resources. The key contributions of this work can be outlined as follows.

- *Vehicular Edge Enabled-Metaverse Architecture:* We propose a collaborative rendering framework based on Metaverse rendering. The framework consists of Metaverse provider server (MPS), roadside units (RSUs), vehicular users, and eavesdroppers. The background elements and foreground objects of virtual scenes are collaboratively rendered by the MPS, the RSUs, and users' local terminals, respectively.
- *Secure and Confidential Communication Scheme:* During the transmission of foreground rendering resources through the uplink, they will be interfered with by eavesdroppers. There, we introduce the secrecy-outage probability (SOP) as a measurement indicator to validate the channel eavesdropping performance. This indicator, rooted in a mathematical probability approach, is defined as the probability that the user-transmitted confidentiality capacity undershoots a pre-defined threshold confidentiality capacity.
- *Hierarchical Joint Optimization Algorithm Mechanism:* Facing the constructed non-convex problem, a hierarchical joint optimization algorithm is proposed to Minimize the Maximum Rendering Latency (MMRL) of vehicular Metaverse rendering system. The offloading strategies, confidentiality interruption strategies, and transmission latencies are optimized separately at each layer.
- *Performance Evaluation:* Through extensive simulation experiments, the system model and algorithms at each layer are evaluated in detail. The results show that the energy consumption of the proposed scheme is significantly lower than other traditional baseline schemes, verifying its effectiveness in reducing latency and energy consumption.

The subsequent sections of this paper are arranged as follows. Section II interprets the relevant works. Section III introduces the architecture of the system model. The problem transformation and proposed algorithms are introduced in Section IV. The simulation results are presented in Section V. Section VI summarizes the entire paper.

II. Literature Review

This section elaborates on the current progress of Metaverse rendering, MEC, multiple access transmission, and Internet of Things security.

i) Metaverse Rendering: In [4], Li et al. proposed the social-aware edge caching framework to solve the problem of providing low-latency and high-quality services. In [3], Xu et al. introduced an edge-device collaborative rendering framework based on real-time computer graphics execution. In [21], Liu et al. investigated a cross-base station collaborative caching mechanism to optimize network resource utilization. In [5], Cheng et al. integrated data correlation and alliance game theory into VR rendering optimization. In [22], Jiang et al. constructed a hierarchical collaborative architecture by integrating coded distributed computing with game theory. In [23], Du et al. proposed an optimal contract design framework predicated on the interaction mechanism between metaverse service providers and network infrastructure, with the primary objective of maximizing the overall utility. In [2], Liu et al. proposed a collaborative VR rendering and dynamic resource leasing mechanism to address high resource consumption. In [24], Ng et al. proposed a stochastic semantic resource allocation scheme to minimize network costs and reduce energy consumption.

ii) Mobile edge computing offloading: In [25], Xu et al. proposed an edge-device collaborative computing framework and separated foreground and background rendering. In [26], Long et al. advocated the algorithm framework and modeled the multi-user Metaverse environment as a graph structure. In [27], Yu et al. designed a framework integrating a digital twin to address physical-digital synchronization in edge resource allocation. In [1], Wang et al. implemented a low-complexity

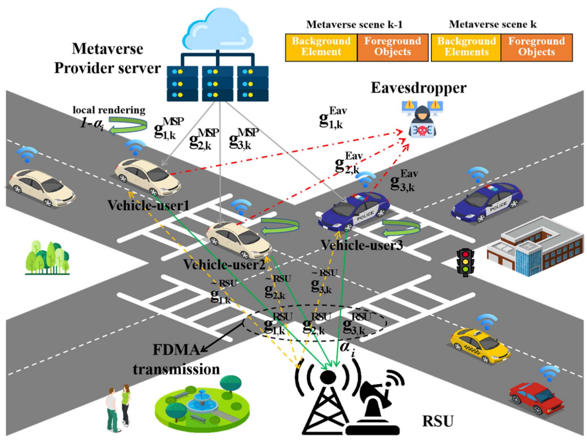

Fig. 1. The scenario of latency-aware Metaverse rendering with resource allocation in vehicular edge networks.

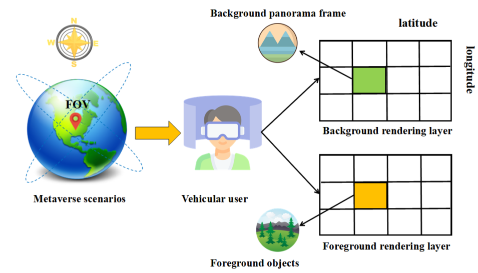

Fig. 2. Metaverse-oriented rendering scene structural diagram.

latency optimization through a greedy task offloading algorithm based on priority. In [28], Li et al. regarded legitimate and illegal devices as multi-agents in reinforcement learning to construct an adversarial game. In [29], Xiao et al. advocated offloading tasks to a fleet queue and introduced consortium blockchain technology. In [30], Yin et al. investigated a hybrid offloading model that coordinates RSUs and shared resource vehicles. In [31], Fan et al. introduced an optimization scheme for a cloud-edge-end collaborative edge computing network with multiple devices and multiple base stations. In [32], Sun et al. introduced a system supporting edge-cloud and edge-edge collaboration to achieve low-latency services. In [33], Sun et al. proposed a three-tier computing architecture to address the issues of task offloading and resource allocation in mobile edge networks for post-disaster rescue scenarios. In [34], Wang et al. studied the offloading, allocation, and caching strategies of edge servers in a three-tier MEC system.

iii) Secrecy resource allocation: In [16], Lu et al. first considered the dynamic threat of flying eavesdroppers in the UAV edge network. In [35], Xing et al. proposed a collaborative intrusion detection framework based on blockchain and an auction game to address the security issues arising from the openness of the Internet of Vehicles. In [17], Gao et al. advocated airships as dynamic eavesdroppers in air-ground networks to construct a confidentiality-energy efficiency optimization model. In [18], Liu et al. designed non-collusive and collusive eavesdropping scenarios to simulate real-world network security threats. In [36], Zhai et al. constructed a Stackelberg game model for three access schemes to improve the overall utility of the system. In [37], Xu et al. proposed a novel non-orthogonal multiple access (NOMA) scheme, which integrates the advantages of time-division multiple access and conventional NOMA. In [12], Wu et al. introduced a NOMA-assisted federated learning scheme to improve the efficiency and stability of model transmission. In [38], Li et al. designed a three-tier MEC architecture and introduced NOMA into the air access network, realizing flexible airborne computing services. In [39], Su et al. proposed a content delivery mechanism to improve service efficiency of vehicle users by jointly optimizing the resource allocation. In [13], Li et al. investigated a dual-path mode to solve the combinatorial optimization problem in multi-user resource allocation. In [40], Wang et al. proposed the diffusion model-based secure sensing system to address the security issue that current research on Integrated Sensing and Communications overlooks the unauthorized sensing of users.

Different from the above related works, we propose a collaborative rendering computation offloading framework based on the vehicular Metaverse and incorporate a channel security assessment mechanism as a key metric into the transmission process. The background panoramic frames are transmitted via frequency division multiple access (FDMA) downlink, while foreground object rendering resources are dynamically and selectively offloaded via FDMA uplink. This scheme not only improves channel resource utilization but also enhances the security performance of the vehicular Metaverse system.

III. System Model and Problem Formulation

A. System Model

As shown in Fig. 1, we consider an immersive experience scene in vehicular Metaverse rendering, which consists of MPS, vehicular users, RSUs, and eavesdroppers. The set of vehicular users is denoted as $\mathcal{I} = \{1, 2, \ldots, I\}$, responding to requests for immersive scene resources $\mathcal{K} = \{1, 2, \ldots, K\}$ from MPS which is responsible for pre-rendering the background elements of virtual scene k. The RSUs are responsible for rendering part of the foreground objects of scene k, and the remaining part is rendered by vehicular terminals. The important symbols used in this paper and their meanings are shown in Table I.

B. Background Rendering Model

As shown in Fig. 2, the Metaverse-oriented rendering scene consists of background panoramic frame and foreground objects. When vehicular user i selects the kth scene of the immersive experience, we use $f^{i,k}_{la,lo}$ to represent the background panorama frames corresponding to different latitudes and longitudes in the scene k requested by the user, parameter $\overline{v}^{i,k}_{la,lo}$ is denoted the average saliency of all pixel points in the frame. The

TABLE I
THE SYMBOLS AND THEIR MEANINGS USED IN THIS PAPER

symbols	Definition
$n^{\text{pix}}_{i,k,o}$	The number of pixels occupied by foreground object o.
$\alpha_{i,k}$	The dynamic offloading ratio for rendering offloaded to RSU.
$\epsilon^{\text{RSU}}_{i,k}$	The security threshold of secrecy outage probability.
μ_i	The local rendering rate of vehicular user i.
$g^{\text{RSU}}_{i,k}$	The channel gain between the vehicular user i and the RSU.
$q^{\text{RSU}}_{i,k}$	The power of vehicular user i for uploading foreground object rendering tasks.
$\hat{W}_i$	Transmission bandwidth for RSU.
$t^{\text{MSP}}_{i,k}$	The latency for vehicular user i to download the background panoramic frame of the kth scene.
$t^{\text{loc}}_{i,k}$	The local rendering latency of vehicular user i.
$t^{\text{tran}}_{i,k}$	The transmission latency for vehicular user i to transmit the rendering tasks of foreground objects.
$t^{\text{loc}}_{i,k,\text{RSU}}$	The latency for RSU to render foreground object tasks with a partial proportion.
$\hat{t}^{\text{tran}}_{i,k}$	The latency for vehicular user i to download the data frames of foreground objects.
$t^{\text{ove}}_{i,k}$	The total rendering latency of vehicular user i.
$E^{\text{loc}}_{i,k}$	The energy consumption generated by local rendering of vehicular user i.
$E^{\text{tran}}_{i,k}$	The energy consumption generated by vehicular user i when uploading foreground object rendering tasks with a partial proportion.
$E^{\text{loc}}_{i,k,\text{RSU}}$	The energy consumption generated by RSU to render foreground object tasks with a partial proportion.

saliency of the background panorama frames can be expressed as

$$\wp(f^{i,k}_{la,lo}) = \frac{\overline{v}^{i,k}_{la,lo}}{\sum_{(\hat{la},\hat{lo})\in\mathcal{L}_k} \overline{v}^{i,k}_{\hat{la},\hat{lo}}}, \quad \forall i\in\mathcal{I}, \forall k\in\mathcal{K}, \tag{1}$$

where parameter $\mathcal{L}_k$ denotes the set of latitudes and longitudes in the kth scene. We assume that the Metaverse virtual scene also follows Zipf's law [3]. Therefore, the popularity of the kth immersive Metaverse scene can be expressed as

$$p^k_i = \left(\sum_{k=1}^{K} R_k^{-\delta}\right)^{-1} / R_k^{\Delta}, \quad \forall i\in\mathcal{I}, \forall k\in\mathcal{K}, \tag{2}$$

where parameter $\Delta \geq 0$ is an important parameter of Zipf's modal law, and parameter R_k is the ranking of the current immersive scene k among the Metaverse server scenes. The popularity of the background panorama frames $p(f^{i,k}_{la,lo})$ is closely related to the popularity of the kth scene p^k_i and the salience of the panorama frames $\wp(f^{i,k}_{la,lo})$, the relationship between them can be specified as

$$p(f^{i,k}_{la,lo}) = p^k_i * \wp(f^{i,k}_{la,lo}) \quad \forall i\in\mathcal{I}, \forall k\in\mathcal{K}. \tag{3}$$

We use $m(f^{i,k}_{la,lo}) \in \{0,1\}$ to determine whether the background elements requested by vehicular user has finished rendering on MPS. If $m(f^{i,k}_{la,lo}) = 0$, it means that the background elements under the location has not been rendered. If $m(f^{i,k}_{la,lo}) = 1$, it means that the background elements under the location has been rendered into background panorama frame and executed on MPS, so the state expression can be specified as

$$m(f^{i,k}_{la,lo}) = \begin{cases} 1, & \text{if the background panorama frame } f^{i,k}_{la,lo} \\ & \text{is executed at MPS,} \\ 0, & \text{otherwise.} \quad \forall i\in\mathcal{I}, \forall k\in\mathcal{K}. \end{cases} \tag{4}$$

In addition, we consider that the total size of the background panorama frames in scene k is $D^{\text{tot}}_{i,k}$, which can be expressed as

$$D^{\text{tot}}_{i,k} = \sum_{(\hat{la},\hat{lo})\in\mathcal{L}_k} m(f^{i,k}_{la,lo}) D(f^{i,k}_{la,lo}), \quad \forall i\in\mathcal{I}, \forall k\in\mathcal{K}, \tag{5}$$

where parameter $D(f^{i,k}_{la,lo})$ denotes the size of the background panorama frames at different positions in scene k. Therefore, the latency for vehicular user i to download the background panoramic frames of the kth scene can be expressed as

$$t^{\text{MPS}}_{i,k} = \frac{\sum_{(\hat{la},\hat{lo})\in\mathcal{L}_k} m(f^{i,k}_{la,lo}) D(f^{i,k}_{la,lo})}{r^{\text{MPS}}_{i,k}}, \forall i\in\mathcal{I}, \forall k\in\mathcal{K}, \tag{6}$$

where parameter $r^{\text{MPS}}_{i,k}$ denotes a transmission rate of background panorama frame between MPS and vehicular user i, which can be specified as

$$r^{\text{MPS}}_{i,k} = W_i \log_2\left(1 + \frac{q^{\text{MPS}}_{i,k} g^{\text{MPS}}_{i,k}}{N_{\text{i}}}\right), \quad \forall i\in\mathcal{I}, \forall k\in\mathcal{K}, \tag{7}$$

where parameter $g^{\text{MPS}}_{i,k}$ denotes the channel gain between MPS and vehicular user i, N_i denotes the Gaussian white noise of the background at the side of vehicular user i, and $q^{\text{MPS}}_{i,k}$ denotes the download power of MPS to vehicular user i, which can be expressed as

$$q^{\text{MPS}}_{i,k} = \frac{N_i}{g^{\text{MPS}}_{i,k}}\left(2^{\frac{D^{\text{tot}}_{i,k}}{W_i t^{\text{MPS}}_{i,k}}} - 1\right), \quad \forall i\in\mathcal{I}, \forall k\in\mathcal{K}. \tag{8}$$

Therefore, the transmission energy consumption of the process can be expressed as

$$\begin{aligned} E^{\text{MPS}}_{i,k} &= q^{\text{MPS}}_{i,k} t^{\text{MPS}}_{i,k} \\ &= \frac{t^{\text{MPS}}_{i,k} N_i}{g^{\text{MPS}}_{i,k}}\left(2^{\frac{D^{\text{tot}}_{i,k}}{W_i t^{\text{MPS}}_{i,k}}} - 1\right), \forall i\in\mathcal{I}, \forall k\in\mathcal{K}. \end{aligned} \tag{9}$$

C. Foreground Object Rendering

Foreground objects requested by vehicular users can be rendered by RSU and their local terminals to enhance the immersive experience. We define $\mathscr{O}^{\text{f}}\{O^{\text{f}}_{i,k,o} | o\in\mathscr{O}^{\text{f}}_{i,k}, i\in\mathcal{I}, k\in\mathcal{K}\}$ as the set of foreground objects in the kth scene within the user's field of view, $S_{i,k,o}$ denotes the data size of the foreground object o in the kth scene within the user's view and it can be expressed as

$$S_{i,k,o} = \theta n^{pix}_{i,k,o}, \forall i\in\mathcal{I}, \forall k\in\mathcal{K}, \tag{10}$$

where parameter θ denotes the bits occupied by each pixel, $n^{\text{pix}}_{i,k,o}$ denotes the number of pixels occupied by the foreground object o in the user's frame. In addition, $n^{\text{pix}}_{i,k,o} = 0$ indicates that the foreground object does not appear within the user's field of view [3]. $\alpha_{i,k}$ represents the proportion of foreground objects rendered by RSU and its data size can be expressed as $\alpha_{i,k}\sum_{o\in O^{\mathrm{f}}_{i,k}} S_{i,k,o}$. The data size of the foreground objects rendered locally is $(1-\alpha_{i,k})\sum_{o\in O^{\mathrm{f}}_{i,k}} S_{i,k,o}$. Therefore, the latency of local rendering on vehicular user i can be expressed as

$$t^{\mathrm{loc}}_{i,k} = \phi_i \frac{(1-\alpha_{i,k})\sum_{o\in O^{\mathrm{f}}_{i,k}} S_{i,k,o}}{\mu_i}, \forall i \in \mathcal{I}, \forall k \in \mathcal{K}, \quad (11)$$

where parameter ϕ_i denotes the number of CPU cycles of vehicular user i, parameter μ_i denotes the local rendering rate of vehicular user i, and the energy consumption generated by the local rendering can be expressed as

$$\begin{aligned} E^{\mathrm{loc}}_{i,k} &= \tau_i \mu_i^3 t^{\mathrm{loc}}_{i,k} \\ &= \tau_i \mu_i^2 \phi_i (1-\alpha_{i,k}) \sum_{o\in O^{\mathrm{f}}_{i,k}} S_{i,k,o}, \forall i \in \mathcal{I}, \forall k \in \mathcal{K}, \quad (12) \end{aligned}$$

where parameter τ_i is the power consumption factor of vehicular user i.

When vehicular user i uploads a portion of the foreground object tasks to RSU for rendering via uplink, the transmission rate can be expressed as

$$r^{\mathrm{RSU}}_{i,k} = \hat{W}_i \log_2\left(1 + \frac{q^{\mathrm{RSU}}_{i,k} g^{\mathrm{RSU}}_{i,k}}{N_{\mathrm{RSU}}}\right), \quad \forall i \in \mathcal{I}, \forall k \in \mathcal{K}, \quad (13)$$

where parameter $\hat{W}_i$ denotes the transmission bandwidth for RSU, parameter $g^{\mathrm{RSU}}_{i,k}$ denotes the channel power gain between vehicular user i and RSU, and parameter N_{RSU} is the background noise at the side of RSU.

The energy consumption of vehicular user i for transmitting a partial proportion of the foreground objects in the kth scene to RSU can be expressed as

$$E^{\mathrm{tran}}_{i,k} = q^{\mathrm{RSU}}_{i,k} t^{\mathrm{tran}}_{i,k}, \quad \forall i \in \mathcal{I}, \forall k \in \mathcal{K}, \quad (14)$$

where parameter $t^{\mathrm{tran}}_{i,k}$ denotes the transmission latency between vehicular user i and RSU for uploading the rendering tasks. After RSU receives them from user i, the rendering latency can be expressed as

$$t^{\mathrm{loc}}_{i,k,\mathrm{RSU}} = \phi_{\mathrm{RSU}} \frac{\alpha_{i,k}\sum_{o\in O^{\mathrm{f}}_{i,k}} S_{i,k,o}}{\mu_{\mathrm{RSU}}}, \quad \forall i \in \mathcal{I}, \forall k \in \mathcal{K}, \quad (15)$$

where parameter μ_{RSU} denotes the rendering rate of RSU. The energy consumption incurred by RSU to render a portion of the foreground objects from the kth scene requested by user i can be expressed as

$$\begin{aligned} E^{\mathrm{loc}}_{i,k,\mathrm{RSU}} &= \tau_{\mathrm{RSU}} \mu_{\mathrm{RSU}}^3 t^{\mathrm{loc}}_{i,k,\mathrm{RSU}} \\ &= \tau_{\mathrm{RSU}} \mu_{\mathrm{RSU}}^2 \phi_{\mathrm{RSU}} \alpha_{i,k} \sum_{o\in O^{\mathrm{f}}_{i,k}} S_{i,k,o}, \quad \forall i \in \mathcal{I}, \forall k \in \mathcal{K}. \quad (16) \end{aligned}$$

The rendered tasks will be returned to vehicular user i in the form of data frames, so that the user can perform subsequent merge operations of the scene. The total size of the foreground object data frames rendered by RSU is denoted $D^{\mathrm{RSU}}_{i,k}$, and the latency for vehicular user i to download them can be expressed as

$$\hat{t}^{\mathrm{tran}}_{i,k} = \frac{D^{\mathrm{RSU}}_{i,k}}{\hat{r}^{\mathrm{RSU}}_{i,k}}, \quad \forall i \in \mathcal{I}, \forall k \in \mathcal{K}, \quad (17)$$

where parameter $\hat{r}^{\mathrm{RSU}}_{i,k}$ denotes the transmission rate at which vehicular user i downloads the foreground data frames rendered by RSU. This rate can be expressed as

$$\hat{r}^{\mathrm{RSU}}_{i,k} = \tilde{W}_i \log_2\left(1 + \frac{\hat{q}^{\mathrm{RSU}}_{i,k} \tilde{g}^{\mathrm{RSU}}_{i,k}}{N_i}\right), \quad \forall i \in \mathcal{I}, \quad \forall k \in \mathcal{K}, \quad (18)$$

where parameter $\tilde{g}^{\mathrm{RSU}}_{i,k}$ is the download link channel gain between RSU and vehicular user i, parameter $\hat{q}^{\mathrm{RSU}}_{i,k}$ denotes the transmission power of the foreground object data frames from RSU to vehicular user i, which can be expressed as

$$\hat{q}^{\mathrm{RSU}}_{i,k} = \frac{N_i}{\tilde{g}^{\mathrm{RSU}}_{i,k}}\left(2^{\frac{D^{\mathrm{RSU}}_{i,k}}{\tilde{W}_i \hat{t}^{\mathrm{tran}}_{i,k}}} - 1\right), \quad \forall i \in \mathcal{I}, \forall k \in \mathcal{K}. \quad (19)$$

Therefore, the energy consumption generated during the download process can be expressed as

$$\hat{E}^{\mathrm{tran}}_{i,k} = \hat{q}^{\mathrm{RSU}}_{i,k} \hat{t}^{\mathrm{tran}}_{i,k}, \quad \forall i \in \mathcal{I}, \quad \forall k \in \mathcal{K}. \quad (20)$$

D. Transmission Model

When user i transmits rendering tasks through the uplink, it may be attacked by eavesdropping attackers. To construct the transmission relationship of illegal information between user i and eavesdropper, we set $g^{\mathrm{Eav}}_{i,k}$ as the channel gain between user i and eavesdropper, and the rate of illegal information transmission between user i and eavesdropper can be expressed as

$$r_{i,\mathrm{Eav}} = \hat{W}_i \log_2\left(1 + \frac{q^{\mathrm{RSU}}_{i,k} g^{\mathrm{Eav}}_{i,k}}{N_{\mathrm{Eav}}}\right), \quad \forall i \in \mathcal{I}, \forall k \in \mathcal{K}, \quad (21)$$

where N_{Eav} denotes the background noise at the side of eavesdropper. Due to the inability to obtain the specific location information of eavesdropper, the channel gain value $g^{\mathrm{Eav}}_{i,k}$ can not be calculated directly through the location information. Here, we will introduce the evaluation metric, which is defined as the probability that the user's transmission secrecy capacity $C^{\mathrm{RSU}}_{i,k}$ is less than the given threshold secrecy capacity $r^{\mathrm{RSU}}_{i,k}$. Its relationship with the transmission power $q^{\mathrm{RSU}}_{i,k}$ and transmission rate $r^{\mathrm{RSU}}_{i,k}$ of the rendered data frames can be expressed as

$$\begin{aligned} & P^{\mathrm{RSU}}_{i,k}(q^{\mathrm{RSU}}_{i,k}, r^{\mathrm{RSU}}_{i,k}) \\ & = 1 - \Pr\left\{ C^{\mathrm{RSU}}_{i,k} \geq r^{\mathrm{RSU}}_{i,k} \,\middle|\, \hat{W}_i \log_2\left(1 + \frac{q^{\mathrm{RSU}}_{i,k} g^{\mathrm{RSU}}_{i,k}}{N_{\mathrm{RSU}}}\right) \right. \\ & \quad \left. \geq \hat{W}_i \log_2\left(1 + \frac{q^{\mathrm{RSU}}_{i,k} g^{\mathrm{Eav}}_{i,k}}{N_{\mathrm{Eav}}}\right) \right\}, \quad \forall i \in \mathcal{I}, \forall k \in \mathcal{K}. \quad (22) \end{aligned}$$

The smaller the value of this metric, the higher the security performance of the immersive rendering model. Among them, the confidentiality capacity of user transmission $C_{i,k}^{\text{RSU}}$ can be expressed as

$$C_{i,k}^{\text{RSU}} = \left[r_{i,k}^{\text{RSU}} - r_{i,k}^{\text{Eav}}\right]^{+}, \forall i \in \mathcal{I}, \forall k \in \mathcal{K}. \tag{23}$$

In order to quantify the impact, we introduce a variable $\epsilon_{i,k}^{\text{RSU}}$ representing the safety threshold of SOP, which means the given value that SOP cannot exceed. This restriction can be expressed as

$$P_{i,k}^{\text{RSU}}(q_{i,k}^{\text{RSU}}, r_{i,k}^{\text{RSU}}) \leq \epsilon_{i,k}^{\text{RSU}}, \forall i \in \mathcal{I}, \forall k \in \mathcal{K}. \tag{24}$$

Therefore, the latency for vehicular user i to transmit the foreground object rendering tasks of the kth scene can be specified as

$$t_{i,k}^{\text{tran}} = \frac{\alpha_{i,k} \sum_{o \in O_{i,k}^{\text{f}}} S_{i,k,o}}{(1-\epsilon_{i,k}^{\text{RSU}}) r_{i,k}^{\text{RSU}}}, \quad \forall i \in \mathcal{I}, \forall k \in \mathcal{K}. \tag{25}$$

Through the following steps, we can obtain $q_{i,k}^{\text{RSU}}$, and then we calculate the energy consumption generated when uploading the rendering tasks of the foreground objects as

$$\begin{aligned} P_{i,k}^{\text{RSU}}(q_{i,k}^{\text{RSU}}, r_{i,k}^{\text{RSU}}) = 1 - \Pr\Bigg\{ & g_{i,k}^{\text{Eav}} \leq \frac{N_{\text{Eav}}}{q_{i,k}^{\text{RSU}}}\left(2^{-\frac{r_{i,k}^{\text{RSU}}}{\hat{W}_i}} - 1\right) \\ & + g_{i,k}^{\text{RSU}} \frac{N_{\text{Eav}}}{N_{\text{RSU}}} 2^{-\frac{r_{i,k}^{\text{RSU}}}{\hat{W}_i}} \,\Big|\, g_{i,k}^{\text{Eav}} \leq g_{i,k}^{\text{RSU}} \frac{N_{\text{Eav}}}{N_{\text{RSU}}} \Bigg\}, \forall i \in \mathcal{I}, \forall k \in \mathcal{K}. \end{aligned} \tag{26}$$

Here, let $\hat{g}_{i,k}^{\text{RSU}} = \frac{N_{\text{Eav}}}{N_{\text{RSU}}} g_{i,k}^{\text{RSU}}$, $\hat{g}_{i,k}^{\text{RSU}}$ can be recognized as the effective channel gain between vehicular user i and RSU. Therefore, (26) can be expressed as

$$\begin{aligned} P_{i,k}^{\text{RSU}}(q_{i,k}^{\text{RSU}}, r_{i,k}^{\text{RSU}}) = 1 - \Pr\Bigg\{ & g_{i,k}^{\text{Eav}} \leq \frac{N_{\text{Eav}}}{q_{i,k}^{\text{RSU}}}\left(2^{-\frac{r_{i,k}^{\text{RSU}}}{\hat{W}_i}} - 1\right) \\ & + \hat{g}_{i,k}^{\text{RSU}} 2^{-\frac{r_{i,k}^{\text{RSU}}}{\hat{W}_i}} \,\Big|\, g_{i,k}^{\text{Eav}} \leq \hat{g}_{i,k}^{\text{RSU}} \Bigg\}, \forall i \in \mathcal{I}, \forall k \in \mathcal{K}. \end{aligned} \tag{27}$$

Based on the above equation, we consider that $g_{i,k}^{\text{Eav}}$ obeys an exponential distribution with a mean value of $\lambda_{i,k}^{\text{Eav}}$. Therefore, it can be solved by using the distribution function and the probability density function of this exponential distribution. Here, $\lambda_{i,k}^{\text{Eav}}$ denotes the average eavesdropping path strength, and the interruption probability can be re-expressed as

$$\begin{aligned} P_{i,k}^{\text{RSU}}\left(q_{i,k}^{\text{RSU}}, r_{i,k}^{\text{RSU}}\right) = & \frac{1}{1 - e^{-\frac{\hat{g}_{i,k}^{\text{RSU}}}{\lambda_{i,k}^{\text{Eav}}}}} \\ & \times \left\{ e^{-\frac{\frac{N_{\text{Eav}}}{q_{i,k}^{\text{RSU}}}\left(2^{-\frac{r_{i,k}^{\text{RSU}}}{\hat{W}_i}} - 1\right) + \frac{N_{\text{Eav}}}{N_{\text{RSU}}} g_{i,k}^{\text{RSU}} 2^{-\frac{r_{i,k}^{\text{RSU}}}{\hat{W}_i}}}{\lambda_{i,k}^{\text{Eav}}}} - e^{-\frac{\hat{g}_{i,k}^{\text{RSU}}}{\lambda_{i,k}^{\text{Eav}}}} \right\}, \\ & \forall i \in \mathcal{I}, k \in \mathcal{K}. \end{aligned} \tag{28}$$

Based on (24) and (28), we can derive

$$\begin{aligned} & \frac{N_{\text{Eav}}}{q_{i,k}^{\text{RSU}}}\left(2^{-\frac{r_{i,k}^{\text{RSU}}}{\hat{W}_i}} - 1\right) + \frac{N_{\text{Eav}}}{N_{\text{RSU}}} g_{i,k}^{\text{RSU}} 2^{-\frac{r_{i,k}^{\text{RSU}}}{\hat{W}_i}} \\ & \geq -\lambda_{i,k}^{\text{Eav}} \ln\left(e^{-\frac{\hat{g}_{i,k}^{\text{RSU}}}{\lambda_{i,k}^{\text{Eav}}}} (1-\epsilon_{i,k}^{\text{RSU}}) + \epsilon_{i,k}^{\text{RSU}} \right), \quad \forall i \in \mathcal{I}, \forall k \in \mathcal{K}. \end{aligned} \tag{29}$$

In addition, an auxiliary variable $\delta_{i,k}^{\text{Eav}}$ is introduced, which is related to the effective channel gain $\hat{g}_{i,k}^{\text{RSU}}$, the average strength of the eavesdropping paths $\lambda_{i,k}^{\text{Eav}}$, and the security threshold of SOP $\epsilon_{i,k}^{\text{RSU}}$, it can be expressed as

$$r_{i,k}^{\text{RSU}} \leq \delta_{i,k}^{\text{Eav}} = -\lambda_{i,k}^{\text{Eav}} \ln\left(e^{-\frac{\hat{g}_{i,k}^{\text{RSU}}}{\lambda_{i,k}^{\text{Eav}}}} (1-\epsilon_{i,k}^{\text{RSU}}) + \epsilon_{i,k}^{\text{RSU}} \right). \tag{30}$$

Based on (29) and (30), the rate at which uploading an immersive foreground object rendering tasks has the following constraints

$$r_{i,k}^{\text{RSU}} \leq \hat{W}_i \log_2\left(\frac{q_{i,k}^{\text{RSU}} \hat{g}_{i,k}^{\text{RSU}} + N_{\text{Eav}}}{q_{i,k}^{\text{RSU}} \delta_{i,k}^{\text{Eav}} + N_{\text{Eav}}} \right), \forall i \in \mathcal{I}, \forall k \in \mathcal{K}. \tag{31}$$

From the analysis of the above equation, it can be concluded that the rate of foreground object uploading is guaranteed to be non-negative only if the effective channel gain $\hat{g}_{i,k}^{\text{RSU}}$ is strictly greater than the auxiliary variable $\delta_{i,k}^{\text{Eav}}$. Additionally, the uploading rate increases with the increase of transmission power, so the transmission rate can be expressed as

$$r_{i,k}^{\text{RSU}} = \hat{W}_i \log_2\left(\frac{q_{i,k}^{\text{RSU}} \hat{g}_{i,k}^{\text{RSU}} + N_{\text{Eav}}}{q_{i,k}^{\text{RSU}} \delta_{i,k}^{\text{Eav}} + N_{\text{Eav}}} \right), \forall i \in \mathcal{I}, \forall k \in \mathcal{K}. \tag{32}$$

The power for uploading immersive foreground object rendering tasks can be solved using the above equation, which is expressed as

$$q_{i,k}^{\text{RSU}} = \frac{N_{\text{Eav}}\left(2^{\frac{r_{i,k}^{\text{RSU}}}{\hat{W}_i}} - 1\right)}{\hat{g}_{i,k}^{\text{RSU}} - \delta_{i,k}^{\text{Eav}} 2^{\frac{r_{i,k}^{\text{RSU}}}{\hat{W}_i}}}, i \in \mathcal{I}, \forall k \in \mathcal{K}. \tag{33}$$

The uploading rate can also be expressed as

$$r_{i,k}^{\text{RSU}} = \frac{\alpha_{i,k} \sum_{o \in O_{i,k}^{\text{f}}} S_{i,k,o}}{t_{i,k}^{\text{tran}}(1-\epsilon_{i,k}^{\text{RSU}})}, \quad \forall i \in \mathcal{I}, \forall k \in \mathcal{K}. \tag{34}$$

Thus, the power for uploading foreground object rendering tasks can be re-expressed as

$$q_{i,k}^{\text{RSU}} = \frac{N_{\text{Eav}}\left(2^{\frac{\alpha_{i,k} \sum_{o \in O_{i,k}^{\text{f}}} S_{i,k,o}}{\hat{W}_i t_{i,k}^{\text{tran}}(1-\epsilon_{i,k}^{\text{RSU}})}} - 1\right)}{\hat{g}_{i,k}^{\text{RSU}} - \delta_{i,k}^{\text{Eav}} 2^{\frac{\alpha_{i,k} \sum_{o \in O_{i,k}^{\text{f}}} S_{i,k,o}}{\hat{W}_i t_{i,k}^{\text{tran}}(1-\epsilon_{i,k}^{\text{RSU}})}}}, \forall i \in \mathcal{I}, \forall k \in \mathcal{K}. \tag{35}$$

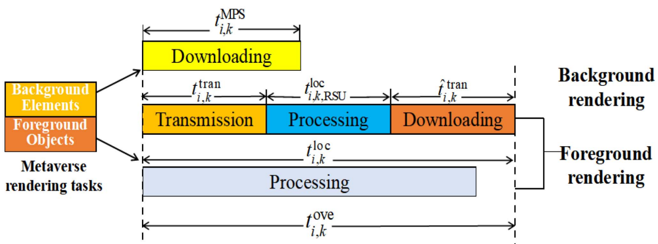

Fig. 3. Rendering latency of vehicular Metaverse.

The energy consumption of vehicular user i for transmitting the foreground objects of the kth scene to RSU can be represented as

$$E^{\rm tran}_{i,k}=\frac{N_{\rm Eav}\left(2^{\frac{\alpha_{i,k}\sum_{o\in O^{\rm f}_{i,k}} S_{i,k,o}}{\hat{W}_i t^{\rm tran}_{i,k}(1-\epsilon^{\rm RSU}_{i,k})}}-1\right)}{\hat{g}^{\rm RSU}_{i,k}-\delta^{\rm Eav}_{i,k}2^{\frac{\alpha_{i,k}\sum_{o\in O^{\rm f}_{i,k}} S_{i,k,o}}{\hat{W}_i t^{\rm tran}_{i,k}(1-\epsilon^{\rm RSU}_{i,k})}}}t^{\rm tran}_{i,k},$$
$$\forall i\in\mathcal{I},\forall k\in\mathcal{K}. \tag{36}$$

The rendering latency of vehicular Metaverse is shown in Fig. 3. The total rendering latency of an immersive rendering model can be expressed as

$$t^{\rm ove}_{i,k}=\max\left\{t^{\rm MPS}_{i,k},\max\left\{t^{\rm loc}_{i,k},t^{\rm tran}_{i,k}+t^{\rm loc}_{i,k,\rm RSU}+\hat{t}^{\rm tran}_{i,k}\right\}\right\},$$
$$\forall i\in\mathcal{I},\forall k\in\mathcal{K}. \tag{37}$$

The total energy consumption of vehicular user i for requesting the kth scene can be expressed as

$$E^{\rm ove}_{i,k}=E^{\rm loc}_{i,k}+E^{\rm tran}_{i,k},\quad \forall i\in\mathcal{I},\quad \forall k\in\mathcal{K}. \tag{38}$$

E. Problem Formulation

Based on the above modeling, this paper constructs a joint optimization problem, aiming to synchronously optimize the offloading strategy $\alpha_{i,k}$, safety threshold of SOP $\epsilon^{\rm RSU}_{i,k}$, and uplink transmission latency of vehicular users $t^{\rm tran}_{i,k}$. Therefore, the objective of the problem is to Minimize the Maximum Rendering Latency (MMRL), which can be expressed as

$$({\rm MMRL}):\min \max_{\forall i\in\mathcal{I},\forall k\in\mathcal{K}}\left\{t^{\rm ove}_{i,k}\right\}$$
$$\text{subject to}:\ 0\le\alpha_{i,k}\le 1,\quad \forall i\in\mathcal{I},\forall k\in\mathcal{K}, \tag{39}$$
$$0\le\epsilon^{\rm RSU}_{i,k}\le 1,\quad \forall i\in\mathcal{I},\forall k\in\mathcal{K}, \tag{40}$$
$$0\le t^{\rm ove}_{i,k}\le T^{\rm max},\quad \forall i\in\mathcal{I},\forall k\in\mathcal{K}, \tag{41}$$
$$0\le E^{\rm ove}_{i,k}\le E^{\rm max},\quad \forall i\in\mathcal{I},\forall k\in\mathcal{K}, \tag{42}$$
$$\text{variables}:\ \alpha_{i,k},\epsilon^{\rm RSU}_{i,k},t^{\rm tran}_{i,k}.$$

In Problem (MMRL), constraint (39) ensures that the offloading ratio does not exceed the total rendering load of foreground objects in the user-requested scene. Constraint (40) ensures the rationality of the security threshold for channel confidentiality outage probability. Constraint (41) ensures that the user's rendering latency does not exceed the maximum time threshold. Constraint (42) ensures that the user's rendering energy consumption does not exceed the maximum energy consumption.

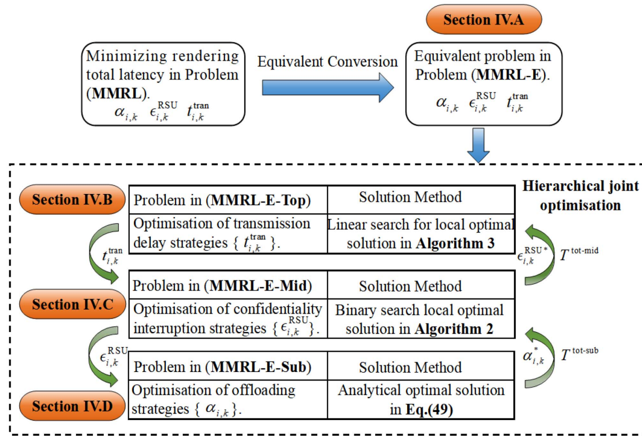

Fig. 4. Hierarchical structure diagram for target optimization.

IV. Hierarchical Solution for Joint Optimization Problems

A. Equivalent Form of Problem (MMRL)

We introduce the parameter $T^{\rm tot}$ to represent the rendering latency corresponding to vehicular user i who completes the rendering tasks last in the vehicular user group $\mathcal{I}$ for immersive experience, which can be expressed as

$$T^{\rm tot}=\max_{\forall i\in\mathcal{I},\forall k\in\mathcal{K}}\left\{t^{\rm ove}_{i,k}\right\}. \tag{43}$$

Based on the introduction of $T^{\rm tot}$, the value range of $\alpha_{i,\rm k}$ can be redefined. Since the latency for users to download the background panoramic frames from MPS is independent of $\alpha_{i,\rm k}$, this part can be ignored. It is only necessary to bring $T^{\rm tot}$ into $t^{\rm loc}_{i,k}$ and $t^{\rm tran}_{i,k}+t^{\rm loc}_{i,k,\rm RSU}+\hat{t}^{\rm tran}_{i,k}$, respectively, to solve $\alpha_{i,\rm k}$. Thus, the range of $\alpha_{i,\rm k}$ can be specified as

$$0\le\alpha_{i,k}\le\min\left\{1-\frac{T^{\rm tot}\mu_i}{\phi_i\sum_{o\in O^{\rm f}_{i,k}}S_{i,k,o}},\right.$$
$$\left.\frac{T^{\rm tot}-t^{\rm tran}_{i,k}-\hat{t}^{\rm tran}_{i,k}}{\phi_{\rm RSU}\sum_{o\in O^{\rm f}_{i,k}}S_{i,k,o}}\mu_{\rm RSU}\right\},\forall i\in\mathcal{I},\forall k\in\mathcal{K}. \tag{44}$$

Based on the above equation, Problem (MMRL) can be equated to

$$\text{(MMRL-E)}:\ \min T^{\rm tot}$$
$$\text{subject to: constraints (40), (41), (42), (44)}$$
$$\text{variables: }\alpha_{i,k},\epsilon^{\rm RSU}_{i,k},t^{\rm tran}_{i,k},T^{\rm tot}.$$

To address the above problem, the issue is decomposed as shown in Fig. 4. With the given values of $\epsilon^{\rm RSU}_{i,k}$ and $t^{\rm tran}_{i,k}$, the underlying problem optimizes the upload ratio of the foreground object rendering tasks and produces the minimum introduction $T^{\rm tot}$.

Thus, the underlying problem can be specified as

$$\begin{aligned}&\text{(MMRL-E-Sub): } \min T^{\text{tot}}\\ &\quad\text{subject to: constraints (42), (44)}\\ &\quad\text{variables: } \alpha_{i,k}, T^{\text{tot}}.\end{aligned}$$

After obtaining T^{tot}, the middle-layer problem will further minimize T^{tot} by adjusting the parameters $\epsilon_{i,k}^{\text{RSU}}$, when given $t_{i,k}^{\text{tran}}$, the middle layer optimize the security threshold of SOP $\epsilon_{i,k}^{\text{RSU}}$, and thus the middle-layer problem can be expressed as

$$\begin{aligned}&\text{(MMRL-E-Mid): } \min T^{\text{tot}}\\ &\quad\text{subject to: constraint (40),}\\ &\quad\text{variables: } \epsilon_{i,k}^{\text{RSU}}.\end{aligned}$$

Based on the above two optimization problems, the top-layer problem will further adjust the upload latency parameter $t_{i,k}^{\text{tran}}$ to minimize T^{tot}, which can be specified as

$$\begin{aligned}&\text{(MMRL-E-Top): } \min T^{\text{tot}}\\ &\quad\text{subject to: constraint (41),}\\ &\quad\text{variables: } t_{i,k}^{\text{tran}}.\end{aligned}$$

B. *Proposed Algorithm for Solving Problem (MMRL-E-Sub)*

In Problem (MMRL-E-Sub), the objective is to minimize the total rendering latency T^{tot}, optimizing the proportion of foreground object rendering tasks under constraint (43). Since the rendering energy consumption decreases as the rendering latency increases, and when the rendering latency tends to infinity, the total rendering energy consumption approaches zero. Therefore, when T^{tot} reaches its maximum value, the sub-problem of minimizing T^{tot} can be equivalent to the problem of minimizing energy consumption, which can be expressed as

$$\begin{aligned}&\text{(MMRL-E-SubCheck): } \min E^{\text{tot}} =\\ &\tau_i\mu_i^2\phi_i(1-\alpha_{i,k})\sum_{o\in O_{i,k}^{\text{f}}} S_{i,k,o} - E^{\max}.\\ &+\frac{N_{\text{Eav}} t_{i,k}^{\text{tran}}\left(2^{\frac{\alpha_{i,k}\sum_{o\in O_{i,k}^{\text{f}}} S_{i,k,o}}{\hat{W}_i t_{i,k}^{\text{tran}}(1-\epsilon_{i,k}^{\text{RSU}})}}-1\right)}{\hat{g}_{i,k}^{\text{RSU}}-\delta_{i,k}^{\text{Eav}} 2^{\frac{\alpha_{i,k}\sum_{o\in O_{i,k}^{\text{f}}} S_{i,k,o}}{\hat{W}_i t_{i,k}^{\text{tran}}(1-\epsilon_{i,k}^{\text{RSU}})}}}.\\ &\quad\text{subject to: constraint (44),}\\ &\quad\text{variables: } \{\alpha_{i,k}\}_{\forall i\in\mathcal{I},\forall k\in\mathcal{K}}.\end{aligned}$$

If Problem (MMRL-E-SubCheck) yields a negative value, it indicates that $E_{i,k}^{\text{ove}} \leq E^{\max}$, satisfying the energy consumption constraint. It shows that the subproblem is feasible, and there exists a non-empty feasible region for $\alpha_{i,k}$ under the given T^{tot}.

Proposition 1: Given the values of $t_{i,k}^{\text{tran}}$, $\epsilon_{i,k}^{\text{RSU}}$, the total energy consumption $\cancel{E^{\text{tot}}}$ of vehicular user i is strict convex with respect to $\alpha_{i,k}$.

Proof: $\mathcal{F}(\alpha_{i,k})$ is defined as the objective function of the problem (MMRL-E-SubCheck). It can be specified as follows.

$$\begin{aligned}\mathcal{F}(\alpha_{i,k}) &= \tau_i\mu_i^2\phi_i(1-\alpha_{i,k})\sum_{o\in O_{i,k}^{\text{f}}} S_{i,k,o} - E^{\max}\\ &+\frac{N_{\text{Eav}} t_{i,k}^{\text{tran}}\left(2^{\frac{\alpha_{i,k}\sum_{o\in O_{i,k}^{\text{f}}} S_{i,k,o}}{\hat{W}_i t_{i,k}^{\text{tran}}(1-\epsilon_{i,k}^{\text{RSU}})}}-1\right)}{\hat{g}_{i,k}^{\text{RSU}}-\delta_{i,k}^{\text{Eav}} 2^{\frac{\alpha_{i,k}\sum_{o\in O_{i,k}^{\text{f}}} S_{i,k,o}}{\hat{W}_i t_{i,k}^{\text{tran}}(1-\epsilon_{i,k}^{\text{RSU}})}}},\\ &\forall i\in\mathcal{I}, \forall k\in\mathcal{K}.\end{aligned} \tag{45}$$

Take the second-order partial derivative of this objective function, we can express it as follows.

$$\begin{aligned}\frac{\partial^2\mathcal{F}(\alpha_{i,k})}{\partial\alpha_{i,k}^2} &= N_{\text{Eav}} t_{i,k}^{\text{tran}}\cdot\left(\frac{\sum_{o\in O_{i,k}^{\text{f}}} S_{i,k,o}}{\hat{W}_i t_{i,k}^{\text{tran}}(1-\epsilon_{i,k}^{\text{RSU}})}\right)^2\\ &\cdot\frac{(\ln 2)^2(\hat{g}_{i,k}^{\text{RSU}}-\delta_{i,k}^{\text{Eav}})\cdot A\cdot(\hat{g}_{i,k}^{\text{RSU}}+\delta_{i,k}^{\text{Eav}}\cdot A)}{(\hat{g}_{i,k}^{\text{RSU}}-\delta_{i,k}^{\text{Eav}}\cdot A)^3},\end{aligned} \tag{46}$$

where A$= 2^{\frac{\alpha_{i,k}\sum_{o\in O_{i,k}^{\text{f}}} S_{i,k,o}}{\hat{W}_i t_{i,k}^{\text{tran}}(1-\epsilon_{i,k}^{\text{RSU}})}}$. Analyzing the derivation results yields that its second order derivative $\frac{\partial^2\mathcal{F}(\alpha_{i,k})}{\partial\alpha_{i,k}^2} \geq 0$. It is proved that Problem (MMRL-E-SubCheck) is strictly convex with respect to $\alpha_{i,k}$. This completes our proof. ■

In order to solve Problem (MMRL-E-SubCheck), the Lagrange function $\mathcal{L}(\alpha_{i,k},\beta,\gamma)$ is constructed by introducing the Lagrange multiplier β, γ by utilizing Karush-Kuhn-Tucker (KKT) method, which can be specified as

$$\begin{aligned}&\mathcal{L}(\alpha_{i,k},\beta,\gamma)\\ &= \tau_i\mu_i^2\phi_i(1-\alpha_{i,k})\sum_{o\in O_{i,k}^{\text{f}}} S_{i,k,o} - E^{\max}\\ &+\frac{N_{\text{Eav}}\left(2^{\frac{\alpha_{i,k}\sum_{o\in O_{i,k}^{\text{f}}} S_{i,k,o}}{\hat{W}_i t_{i,k}^{\text{tran}}(1-\epsilon_{i,k}^{\text{RSU}})}}-1\right)}{\hat{g}_{i,k}^{\text{RSU}}-\delta_{i,k}^{\text{Eav}} 2^{\frac{\alpha_{i,k}\sum_{o\in O_{i,k}^{\text{f}}} S_{i,k,o}}{\hat{W}_i t_{i,k}^{\text{tran}}(1-\epsilon_{i,k}^{\text{RSU}})}}} t_{i,k}^{\text{tran}} - \beta\alpha_{i,k}\\ &+\gamma(\alpha_{i,k}-B),\end{aligned} \tag{47}$$

where $B = \min\{1-\frac{T^{\text{tot}}\mu_i}{\phi_i\sum_{o\in O_{i,k}^{\text{f}}} S_{i,k,o}}, \frac{T^{\text{tot}}-t_{i,k}^{\text{tran}}-\hat{t}_{i,k}^{\text{tran}}}{\phi_{\text{RSU}}\sum_{o\in O_{i,k}^{\text{f}}} S_{i,k,o}}\mu_{\text{RSU}}\}$.

The first-order partial derivation of Lagrange function $\mathcal{L}(\alpha_{i,k},\beta,\gamma)$ to $\alpha_{i,k}$ is expressed as follows

$$\begin{aligned}\frac{\partial\mathcal{L}(\alpha_{i,k},\beta,\gamma)}{\partial\alpha_{i,k}} &= -\tau_i\mu_i^2\phi_i\sum_{o\in O_{i,k}^{\text{f}}} S_{i,k,o}\\ &+ N_{\text{Eav}} t_{i,k}^{\text{tran}}\frac{\sum_{o\in O_{i,k}^{\text{f}}} S_{i,k,o}}{\hat{W}_i t_{i,k}^{\text{tran}}(1-\epsilon_{i,k}^{\text{RSU}})}\cdot\frac{A\cdot\ln 2(\hat{g}_{i,k}^{\text{RSU}}-\delta_{i,k}^{\text{Eav}})}{(\hat{g}_{i,k}^{\text{RSU}}-\delta_{i,k}^{\text{Eav}}\cdot A)^2}\end{aligned}$$

$$-\beta+\gamma,\quad \forall i\in\mathcal{I},\quad \forall k\in\mathcal{K}. \tag{48}$$

Let the first-order derivative $\frac{\partial\mathcal{L}(\alpha_{i,k},\beta,\gamma)}{\partial\alpha_{i,k}}=0$, the uploading ratio of the rendering tasks for the immersive foreground objects can be expressed as (49) shown at the bottom of this page, where $c_1=\frac{N_{\text{Eav}}\sum_{o\in O^{\text{f}}_{i,k}}S_{i,k,o}}{\hat{W}_i(1-\epsilon^{\text{RSU}}_{i,k})}$, $c_2=\hat{g}^{\text{RSU}}_{i,k}$, $c_3=\delta^{\text{Eav}}_{i,k}$, $K=-\tau_i\mu_i^2\phi_i\sum_{o\in O^{\text{f}}_{i,k}}S_{i,k,o}-\beta+\gamma$.

Through the analysis of Problem (MMRL-E-SubCheck), it can be found that when T^{tot} is given, if $E^{\text{tot}}\le 0$, it means that the energy consumption meets the requirement, and the value of T^{tot} can be further reduced, otherwise it should be increased. In addition, the objective function decreases as T^{tot} increases. Based on this characteristic, the pairwise search method can be used to solve the sub-problem (MMRL-E-Sub) in the interval $[0,T^{\max}]$. The specific steps are as Algorithm 1.

- *Step 1-Step 2:* First, we randomly assign two values to $t^{\text{tran}}_{i,k}$, $\epsilon^{\text{RSU}}_{i,k}$ and give the small computation-error η. Then we initialize the current optimal upload ratio $\alpha^*_{i,k}=\emptyset$, the current optimal objective function value $E^{\text{tot-cur}}=\infty$, the lower bound and upper bound of T^{tot} as $T^{\text{tot-lb}}=0$ and $T^{\text{tot-ub}}=T^{\max}$.
- *Step 3-Step 15:* Firstly, we calculate the current total rendering delay $T^{\text{tot-cur}}$ by using the bisection method. Secondly, we derive the optimal offloading strategy for rendering resources by invoking Formula (49) shown at the bottom of next page, and substitute it into Formula (45) to calculate the corresponding energy consumption. Then, we compare this energy consumption with the current optimal energy consumption $E^{\text{tot-cur}}$. Finally, we determine whether this energy consumption is less than 0. If $E^{\text{tot}}(\alpha^*_{i,k})<0$, we update $T^{\text{tot-ub}}=T^{\text{tot-cur}}$, otherwise, we update $T^{\text{tot-lb}}=T^{\text{tot-cur}}$.
- *Step 16:* We assign the value of $E^{\text{tot-cur}}$ to $E^{\text{tot}}(\alpha^*_{i,k})^*$ and derive the optimal task offloading strategy $\alpha_{i,k}{}^*$.

Proposition 2: Given the value of $t^{\text{tran}}_{i,k}$, the total energy consumption $E^{\text{tot}}_{i,k}$ of vehicular user i is increasing with the safety threshold of SOP $\epsilon^{\text{RSU}}_{i,k}$.

Proof: In the paper, $\mathcal{F}(\epsilon^{\text{RSU}}_{i,k})$ is defined as the objective function of Problem (MMRL-E-SubCheck). It can be specified as

$$\mathcal{F}(\epsilon^{\text{RSU}}_{i,k})=\tau_i\mu_i^2\phi_i(1-\alpha_{i,k})\sum_{o\in O^{\text{f}}_{i,k}}S_{i,k,o}-E^{\max}+\frac{N_{\text{Eav}}t^{\text{tran}}_{i,k}\left(2^{\frac{\alpha_{i,k}\sum_{o\in O^{\text{f}}_{i,k}}S_{i,k,o}}{\hat{W}_i t^{\text{tran}}_{i,k}(1-\epsilon^{\text{RSU}}_{i,k})}}-1\right)}{\hat{g}^{\text{RSU}}_{i,k}-\delta^{\text{Eav}}_{i,k}2^{\frac{\alpha_{i,k}\sum_{o\in O^{\text{f}}_{i,k}}S_{i,k,o}}{\hat{W}_i t^{\text{tran}}_{i,k}(1-\epsilon^{\text{RSU}}_{i,k})}}},$$
$$\forall i\in\mathcal{I},\forall k\in\mathcal{K}. \tag{50}$$

Algorithm 1: Proposed Algorithm for Obtaining the Optimal Offloading Ratio in Problem (MMRL-E-Sub).

1: **Input:** $t^{\text{tran}}_{i,k}$, $\epsilon^{\text{RSU}}_{i,k}$. The computation error η as a minimal value.
2: **Initialization:** Initialize the current optimal upload ratio $\alpha^*_{i,k}=\emptyset$ and the current optimal objective function value $E^{\text{tot-cur}}=\infty$, the lower bound and upper bound of T^{tot} as $T^{\text{tot-lb}}$=0 and $T^{\text{tot-ub}}=T^{\max}$.
3: **while** $\eta\le|T^{\text{tot-ub}}-T^{\text{tot-lb}}|$ **do**
4: Calculate the current value as $T^{\text{tot-cur}}=\frac{T^{\text{tot-lb}}+T^{\text{tot-ub}}}{2}$.
5: Invoke (49) to obtain the value of $\alpha^*_{i,k}$.
6: Invoke (45) to obtain the value of $E^{\text{tot}}(\alpha^*_{i,k})$.
7: **if** $E^{\text{tot}}(\alpha^*_{i,k})\le E^{\text{tot-cur}}$ **then**
8: Set $E^{\text{tot-cur}}=E^{\text{tot}}(\alpha^*_{i,k})$ and update the current optimal upload ratio of $\alpha^*_{i,k}$.
9: **end if**
10: **if** $E^{\text{tot}}(\alpha^*_{i,k})<0$ **then**
11: Set $T^{\text{tot-ub}}=T^{\text{tot-cur}}$.
12: **else**
13: Set $T^{\text{tot-lb}}=T^{\text{tot-cur}}$.
14: **end if**
15: **end while**
16: **Output:** The optimal value $E^{\text{tot}}(\alpha^*_{i,k})^*=E^{\text{tot-cur}}$, the optimal value of $T^{\text{tot-sub}*}=T^{\text{tot-cur}}$, and the optimal offloading strategy $\alpha^*_{i,k}$.

We take the first-order partial derivative of this objective function as

$$\frac{\partial\mathcal{F}(\epsilon^{\text{RSU}}_{i,k})}{\partial\epsilon^{\text{RSU}}_{i,k}}=\frac{N_{\text{Eav}}\alpha_{i,k}\sum_{o\in O^{\text{f}}_{i,k}}S_{i,k,o}\ln 2(\hat{g}^{\text{RSU}}_{i,k}-\delta^{\text{Eav}}_{i,k})2^x}{\hat{W}_i(1-\epsilon^{\text{RSU}}_{i,k})^2(\hat{g}^{\text{RSU}}_{i,k}-\delta^{\text{Eav}}_{i,k}2^x)^2}, \tag{51}$$

where $x=\frac{\alpha_{i,k}\sum_{o\in O^{\text{f}}_{i,k}}S_{i,k,o}}{\hat{W}_i t^{\text{tran}}_{i,k}(1-\epsilon^{\text{RSU}}_{i,k})}$. Analyzing the derivation results yields that its first order derivative $\frac{\partial\mathcal{F}(\epsilon^{\text{RSU}}_{i,k})}{\partial\epsilon^{\text{RSU}}_{i,k}}\ge 0$. It is proved that Problem (MMRL-E-SubCheck) is strictly monotonic for $\epsilon^{\text{RSU}}_{i,k}$. This completes our proof. ■

C. Proposed Algorithm for Solving Problem (MMRL-E-Mid)

Through the analysis of sub-problem (WWRL-E-Sub), we derive the optimal offloading ratio of foreground object rendering tasks $\alpha_{i,k}{}^*$ and the corresponding $T^{\text{tot-sub}*}$. In the middle-layer Problem (MMRL-E-Mid), the value of $T^{\text{tot-sub}*}$ is further optimized by adjusting the safety threshold of SOP $\epsilon^{\text{RSU}}_{i,k}$. However, the analytical solution of $\epsilon^{\text{RSU}}_{i,k}$ cannot be derived from the objective function. Therefore, the partial derivative of the objective function with respect to the variable parameter $\epsilon^{\text{RSU}}_{i,k}$ can be calculated to observe its monotonicity. The minimum value of the objective function can be found using the binary

$$\alpha^*_{i,k}=\frac{\hat{W}_i t^{\text{tran}}_{i,k}(1-\epsilon^{\text{RSU}}_{i,k})}{\sum_{o\in O^{\text{f}}_{i,k}}S_{i,k,o}}\log_2\left(\frac{-(c_1\ln 2(c_2-c_3)-2Kc_2c_3)\pm\sqrt{(c_1\ln 2(c_2-c_3)-2Kc_2c_3)^2-4Kc_3^2\cdot Kc_2^2}}{2Kc_3^2}\right) \tag{49}$$

search method under constraint (39), and we can obtain the optimal safety threshold of SOP $\epsilon_{i,k}^{\text{RSU}*}$. The specific steps are as follows.

- *Step 1-Step 2:* Firstly, we randomly assign one value to $t_{i,k}^{\text{tran}}$, and set the lower bound $\epsilon_{i,k}^{\text{RSU-lb}} = 0$, the upper bound of $\epsilon_{i,k}^{\text{RSU-ub}} = 1$. We set the calculation precision as a minimal value ϖ. Then, we initialize the current optimal secrecy outage strategy $\epsilon_{i,k}^{\text{RSU}*} = \emptyset$ and the current optimal objective function value $T^{\text{tot-cur}} = \infty$.
- *Step 3-Step 7:* We search for the safety threshold of SOP within the interval [0, 1] using the bisection search method, aiming to find the optimal secrecy strategy. Then, we calculate the current security threshold $\epsilon_{i,k}^{\text{RSU-mid}}$ and the midpoints of its left and right intervals, respectively, and substitute them into Algorithm 1 to obtain the corresponding $E^{\text{tot-mid}}(\epsilon_{i,k}^{\text{RSU-left}})$, $E^{\text{tot-left}}(\epsilon_{i,k}^{\text{RSU-mid}})$, $E^{\text{tot-right}}(\epsilon_{i,k}^{\text{RSU-right}})$.
- *Step 8-Step 17:* We update the search interval by judging the magnitude of energy. If $E^{\text{tot-left}} < E^{\text{tot-mid}}$, we update the upper bound $\epsilon_{i,k}^{\text{RSU-ub}} = \epsilon_{i,k}^{\text{RSU-mid}}$. If $E^{\text{tot-right}} < E^{\text{tot-mid}}$, we update the lower bound of $\epsilon_{i,k}^{\text{RSU-lb}} = \epsilon_{i,k}^{\text{RSU-mid}}$.
- *Step 18-Step 23:* We obtain $T^{\text{tot-sub}*}$ by invoking Algorithm 1 and compare it with the current optimal value of the objective function $T^{\text{tot-cur}}$. If $T^{\text{tot-sub}*} < T^{\text{tot-cur}}$, we update $T^{\text{tot-cur}} = T^{\text{tot-sub}*}$ and $\epsilon_{i,k}^{\text{RSU}*} = \cancel{T^{\text{tot-cur}}}$. Finally, we assign the value of $T^{\text{tot-cur}}$ to $T^{\text{tot-mid}*}$ and derive the optimal secrecy interruption strategy $\epsilon_{i,k}^{\text{RSU}*}$.

D. Proposed Algorithm for Solving Problem (MMRL-E-Top)

Through the analysis of Problem (MMRL-E-Mid), we obtain the optimal safety threshold of SOP $\epsilon_{i,k}^{\text{RSU}*}$ and the corresponding $T^{\text{tot-mid}*}$. In the top-layer Problem (MMRL-E-Top), $T^{\text{tot-mid}*}$ is further optimized to its minimum by adjusting $t_{i,k}^{\text{tran}}$. Similar to the middle-layer problem, since the analytical solution cannot be derived, a linear search method is used to find the minimum $T^{\text{tot-top}*}$ and derive the optimal transmission strategy $t_{i,k}^{\text{tran}*}$. The specific steps are as follows.

- *Step 1-Step 2:* Firstly, we set the lower bound of $t_{i,k}^{\text{tran}} = 0$, the upper bound of $t_{i,k}^{\text{tran}} = T^{\max}$, and the step size $\Delta t_{i,k}^{\text{tran}}$ for updating the values of $t_{i,k}^{\text{tran}}$. Then, we initialize the current best transmission strategy $t_{i,k}^{\text{tran}*} = \emptyset$ and the current optimal objective function value $T^{\text{tot-cur}} = \infty$.
- *Step 3-Step 9:* We use the linear search method to search the transmission delay within the interval $[0 - T^{\max}]$. Then, we invoke Algorithm 2 to obtain the value of $T^{\text{tot-mid}*}$ and compare it with the current optimal objective function value $T^{\text{tot-cur}}$. If $T^{\text{tot-mid}*} < T^{\text{tot-cur}}$, we update $T^{\text{tot-cur}} = T^{\text{tot-mid}*}$ and $t_{i,k}^{\text{tran}*} = t_{i,k}^{\text{tran-lb}}$. Finally, we assign the value of $T^{\text{tot-cur}}$ to $T^{\text{tot-top}*}$ and derive the optimal transmission strategy.

V. Experimental Design and Results

A. Simulation Setup

In the simulation scenario, we consider five vehicular users distributed within a 5 km $\times$ 5 km area. The total amount of

Algorithm 2: Binary Search Algorithm for Searching the Optimal Confidentiality Security Threshold in Problem (MMRL-E-Mid).

1: **Input:** $t_{i,k}^{\text{tran}}$, the lower bound and the upper bound of $\epsilon_{i,k}^{\text{RSU}}$ as a small value $\epsilon_{i,k}^{\text{RSU-lb}}$ and a large value $\epsilon_{i,k}^{\text{RSU-ub}}$. The calculation precision as a minimal value ϖ.
2: **Initialization:** Initialize the current optimal confidentiality security threshold $\epsilon_{i,k}^{\text{RSU}*} = \emptyset$ and the current optimal objective function value $T^{\text{tot-cur}} = \infty$.
3: **while** $\varpi \le |\epsilon_{i,k}^{\text{RSU-ub}} - \epsilon_{i,k}^{\text{RSU-lb}}|$ **do**
4:     Calculate the current value as $\epsilon_{i,k}^{\text{RSU-mid}} = \frac{\epsilon_{i,k}^{\text{RSU-lb}} + \epsilon_{i,k}^{\text{RSU-ub}}}{2}$.
5:     Calculate the middle point value of the left interval as $\epsilon_{i,k}^{\text{RSU-left}} = \epsilon_{i,k}^{\text{RSU-lb}} + \frac{\epsilon_{i,k}^{\text{RSU-mid}} - \epsilon_{i,k}^{\text{RSU-lb}}}{2}$.
6:     Calculate the middle point value of the right interval as $\epsilon_{i,k}^{\text{RSU-right}} = \epsilon_{i,k}^{\text{RSU-mid}} + \frac{\epsilon_{i,k}^{\text{RSU-ub}} - \epsilon_{i,k}^{\text{RSU-mid}}}{2}$.
7:     Invoking (45) to obtain the values of $E^{\text{tot-mid}}(\alpha_{i,k}^{*}, \epsilon_{i,k}^{\text{RSU-left}})$, $E^{\text{tot-left}}(\alpha_{i,k}^{*}, \epsilon_{i,k}^{\text{RSU-mid}})$, $E^{\text{tot-right}}(\alpha_{i,k}^{*}, \epsilon_{i,k}^{\text{RSU-right}})$.
8:     **if** $E^{\text{tot-left}} < E^{\text{tot-mid}}$ **then**
9:         $\epsilon_{i,k}^{\text{RSU-ub}} = \epsilon_{i,k}^{\text{RSU-mid}}$.
10:     **else**
11:         **if** $E^{\text{tot-right}} < E^{\text{tot-mid}}$ **then**
12:             $\epsilon_{i,k}^{\text{RSU-lb}} = \epsilon_{i,k}^{\text{RSU-mid}}$.
13:         **else**
14:             $\epsilon_{i,k}^{\text{RSU-lb}} = \epsilon_{i,k}^{\text{RSU-left}}$.
15:             $\epsilon_{i,k}^{\text{RSU-ub}} = \epsilon_{i,k}^{\text{RSU-right}}$.
16:         **end if**
17:     **end if**
18:     Invoking Algorithm 1 to obtain the value of $T^{\text{tot-sub}*}$.
19:     **if** $T^{\text{tot-sub}*} < T^{\text{tot-cur}}$ **then**
20:         $T^{\text{tot-cur}} = T^{\text{tot-sub}*}$, $\epsilon_{i,k}^{\text{RSU}*} = \cancel{T^{\text{tot-cur}}}$.
21:     **end if**
22: **end while**
23: **Output:** The optimal value as $T^{\text{tot-mid}*} = T^{\text{tot-cur}}$, and the optimal security strategy $\epsilon_{i,k}^{\text{RSU}*} = \epsilon_{i,k}^{\text{RSU-mid}}$.

rendering tasks for foreground objects is in the interval of [4, 12] Mbytes. The maximum rendering rate of RSU and vehicular user i are set as 1.65×10^{10} cycles/ms and 1.45×10^{10} cycles/ms. Other parameters of the simulation are shown in Table II. To verify the effectiveness and superiority of the proposed algorithm, we compare it with the following baseline methods.

- *Zero Offloading Scheme:* All foreground object rendering resources are rendered by the local terminals of the vehicular users.
- *Fixed Offloading Scheme:* Vehicular users upload rendering resources of foreground objects in their requested scenes to RSU via FDMA transmission.
- *Simulated Annealing:* It is a general global optimization algorithm that uses "temperature" as a control parameter.

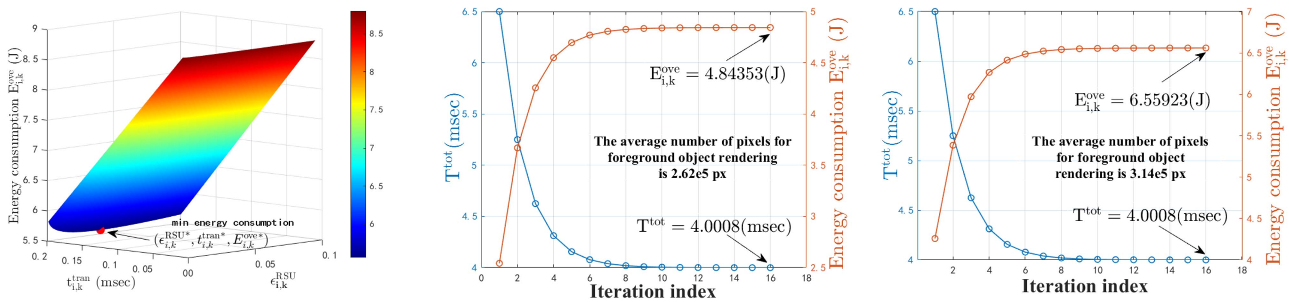

(a) (b) (c)

Fig. 5. Performance evaluation of the proposed algorithm in solving the Problem (MMRL) under the condition of fixed $E^{\max} = 15$ J. (a) Visualization of three dimensional energy consumption distribution based on $\epsilon^{\text{RSU}}_{i,k}$ and $t^{\text{tran}}_{i,k}$. (b) Explanation of our proposed algorithm applied to solving Problem (MMRL) when $n^{\text{pix}}_{i,k,o} = 2.62\text{e}5\text{px}$. (c) Explanation of our proposed algorithm applied to solving Problem (MMRL) when $n^{\text{pix}}_{i,k,o} = 3.14\text{e}5\text{px}$.

Algorithm 3: Linear Search Algorithm for Searching the Optimal Transmission Latency in Problem (MMRL-E-Top).

Input: The lower and upper bound of $t^{\text{tran}}_{i,k}$ as $t^{\text{tran-lb}}_{i,k} = 0$ and $t^{\text{tran-ub}}_{i,k} = T^{\max}$. The step size $\Delta t^{\text{tran}}_{i,k}$ for updating the values of $t^{\text{tran}}_{i,k}$.
Initialization: Initialize the current best transmission strategy $t^{\text{tran}*}_{i,k} = \emptyset$ and the current optimal objective function value $T^{\text{tot-cur}} = \infty$.
for $t^{\text{tran-lb}}_{i,k}$; $t^{\text{tran-lb}}_{i,k} < t^{\text{tran-ub}}_{i,k}$; $t^{\text{tran-lb}}_{i,k} + \Delta t^{\text{tran}}_{i,k}$ **do**
    Invoking Algorithm 2 to obtain the value of $T^{\text{tot-mid}*}$.
    if $T^{\text{tot-mid}*} < T^{\text{tot-cur}}$ **then**
        $T^{\text{tot-cur}} = T^{\text{tot-mid}*}$, and $t^{\text{tran}*}_{i,k} = t^{\text{tran-lb}}_{i,k}$.
    end if
end for
Output: The optimal value as $T^{\text{tot-top}*} = T^{\text{tot-cur}}$, and the optimal transmission strategy $t^{\text{tran}*}_{i,k}$.

TABLE II
PARAMETERS USED IN OUR SIMULATIONS

Parameters	Values
The rendering rate of RSU, μ_{RSU}	1.65e10 cycles/ms
The number of CPU cycles for processing one bit of data by RSU, ϕ_{RSU}	3e10cycles
The power consumption factor coefficient of vehicular user i, τ_i	4e − 20
The power consumption factor coefficient of RSU, τ_{RSU}	1e − 23
The Gaussian white background noise of vehicular user i, N_i	1e − 9dBm
The Gaussian white background noise of eavesdropper, N_{Eav}	1e − 9dBm
The Gaussian white background noise of RSU, N_{RSU}	1e − 12dBm
The number of bits occupied by each pixel point of the foreground objects, θ	32bits
The averag eavesdropping-path strength, λ_{Eav}	1e − 9

B. Simulation Results and Evaluation

Fig. 5 illustrates the performance evaluation of the proposed algorithms in solving Problem (MMRL) under the condition of fixed $E^{\max} = 15$ J. Fig. 5(a) illustrates the three-dimensional distribution among the minimum energy consumption of vehicular user, the security threshold of SOP, and the transmission latency. Logically verifies the feasibility and effectiveness of the hierarchical joint optimization algorithm proposed in this paper in solving Problem (MMRL). Fig. 5(b) and ~~5(c)~~ exhibit that both the minimum latency T^{tot} and corresponding energy consumption $E^{\text{ove}}_{i,k}$ converge to a fixed value, respectively, when all vehicular users complete their rendering tasks in vehicular immersive rendering system. It can be seen that the proposed scheme can obtain the optimal solution for minimizing total delay T^{tot} under the constraint of maximum energy consumption of vehicular users within a limited number of iterations.

Fig. 6 illustrates the relationship between the energy consumption and the optimal confidential interruption strategy under different vehicular users, different transmission latencies, and different numbers of pixels. Fig. 6(a) shows the variation in energy consumption among different users as a function of the safety threshold of SOP in vehicular immersive rendering system. Fig. 6(a) indicates that all users can search for their respective optimal safety threshold of SOP within a limited number of iterations, demonstrating the effectiveness and efficiency of the proposed algorithm in obtaining optimal solutions. Fig. 6(b) shows the relationship between the security threshold of SOP and energy consumption for vehicular user i at different pixel counts. As shown in Fig. 6(b), as the number of pixels increases, the energy consumption of vehicular users increases. This is because high-resolution foreground objects require more rendering resources and energy consumption to achieve real-time rendering. Fig. 6(c) shows the relationship between the safety threshold of SOP and energy consumption for vehicular user i at different transmission latencies. As shown in Fig. 6(c), as the transmission latency increases, the energy consumption decreases. This is because when the transmission latency approaches infinity, the energy consumption generated during the transmission process tends to zero.

Fig. 7 illustrates the relationship between energy consumption and transmission latency, different numbers of pixels, different channel gains, and different channel bandwidths. Fig. 7(a) shows the relationship between transmission latency and energy consumption for vehicular user i under different numbers of

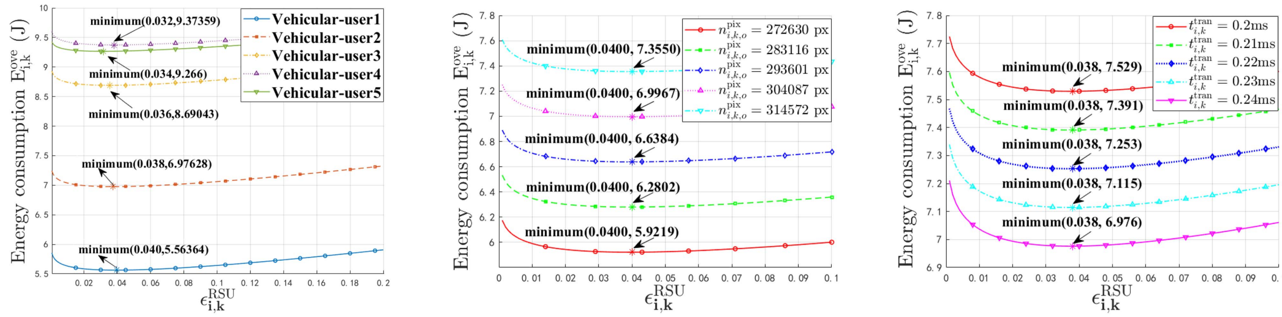

(a) (b) (c)

Fig. 6. The relationship between energy consumption and secrecy-outage probability threshold under different conditions. (a) Change diagram of energy consumption with different secrecy-outage probability thresholds under varying vehicular users. (b) Change diagram of energy consumption with different secrecy-outage probability thresholds under varying numbers of pixels. (c) Change diagram of energy consumption with different secrecy-outage probability thresholds under varying transmission latencies.

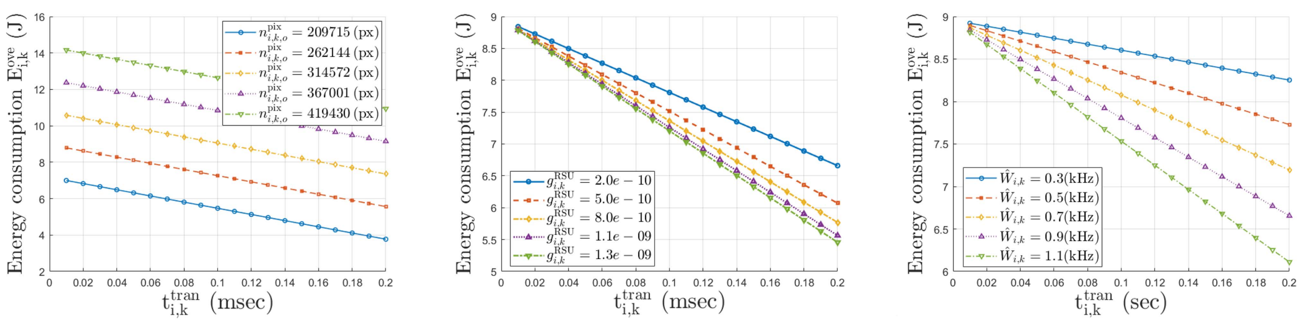

(a) (b) (c)

Fig. 7. The relationship between energy consumption and transmission latency under different conditions. (a) Change diagram of energy consumption with different transmission latencies under varying numbers of pixels. (b) Change diagram of energy consumption with different transmission latencies under varying channel gains. (c) Change diagram of energy consumption with different transmission latencies under varying channel bandwidths.

pixels. As shown in Fig. 7(a), for the same number of pixels, as the transmission latency increases, the energy consumption of the user system decreases. This is because when transmission latency approaches infinity, the energy consumption generated during the transmission process gradually approaches zero. Additionally, it can be observed that the larger the number of pixels in the foreground objects being rendered, the greater the user energy consumption. Fig. 7(b) and ~~7(c)~~ show the variation diagrams of transmission latency and energy consumption for vehicular user i under different channel gains and different channel bandwidths, respectively. As can be seen from Fig. 7(b) and ~~7(c)~~ for the same transmission latency, the larger the channel gain or channel bandwidth occupied in the uplink transmission process, the smaller energy consumption. This is because the better channel conditions mean that the channel has a stronger ability to transmit equal amounts of rendering resources per unit time, thus reducing the energy consumption of the user.

Fig. 8 demonstrates the comparison of energy consumption generated by vehicular users during immersive experience requests between the proposed scheme and baseline schemes. Fig. 8(a) shows the energy consumption comparison between the proposed algorithm and baseline algorithms in terms of the number of foreground object pixels. Compared with other baseline algorithms, the proposal can reduce the energy consumption generated by vehicular users during real-time requests for Metaverse scenes to a certain extent. This is because the scheme simultaneously considers the optimal offloading strategy, optimal secrecy strategy, and optimal transmission latency formulation strategy, thereby minimizing the energy consumption of vehicular users. Fig. 8(b) and ~~8(c)~~ show the energy consumption comparisons between the proposed algorithm and baseline algorithms in terms of the security threshold of the SOP and transmission latency, respectively. The experimental results verify the effectiveness of the proposed algorithm in minimizing the total rendering latency and energy consumption of the vehicular Metaverse system.

Fig. 9 demonstrates the comparison of energy consumption between the proposed scheme and different baseline schemes under different channel conditions. Fig. 9(a) and ~~9(b)~~ show the energy consumption comparisons between the proposed algorithm and the benchmark algorithms in terms of transmission bandwidth and channel gain, respectively. Compared with other benchmark algorithms, the proposal can significantly reduce the energy consumption.

Fig. 10 and ~~11~~ show a comparison of the accuracy of obtaining optimal solutions and computational performance

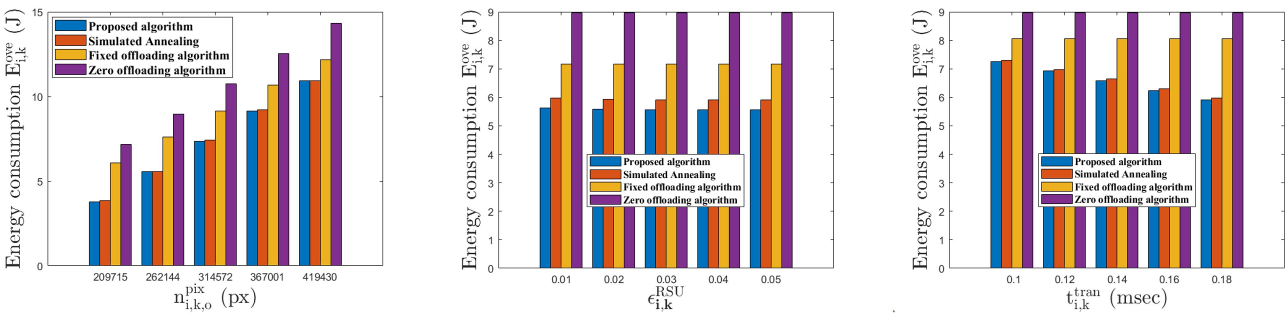

(a) (b) (c)

Fig. 8. Energy consumption comparison between the proposed scheme and different baseline schemes under different conditions. (a) Comparison diagram of energy consumption with numbers of pixels under different schemes. (b) Comparison diagram of energy consumption with secrecy-outage probability thresholds under different schemes. (c) Comparison diagram of energy consumption with transmission latencies under different schemes.

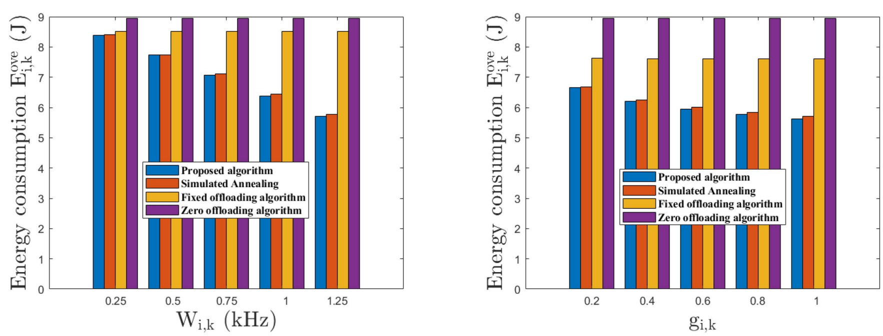

(a) (b)

Fig. 9. Energy consumption comparison between the proposed scheme and different baseline schemes under different channel conditions. (a) Comparison diagram of energy consumption with bandwidths under different schemes. (b) Comparison diagram of energy consumption with channel gains under different schemes.

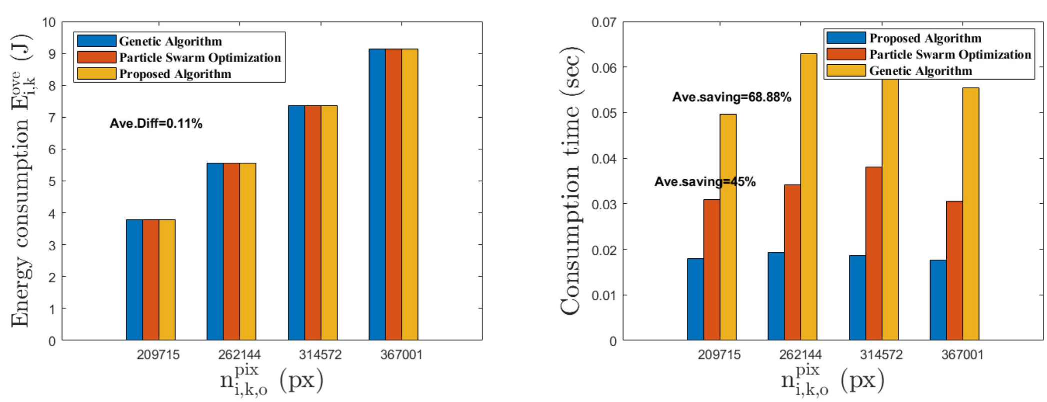

(a) (b)

Fig. 10. Comparison of the proposed algorithm and the baseline algorithms in searching for local optimal solutions and computational efficiency. (a) Comparison between the proposed algorithm and the baseline algorithms for searching local optimal solutions under varying numbers of pixels. (b) Comparison of the computational efficiency of the proposed algorithm and the baseline algorithms under varying numbers of pixels.

between the proposed algorithm and commonly used algorithms for solving non-convex problems, such as genetic algorithms and particle swarm algorithms. As shown in Fig. 10, compared with the two base algorithms, the difference in the optimal solution for energy consumption is 0.11%. However, in terms of computational performance, the proposal can significantly improve computational efficiency, with an improvement of 69% compared to the genetic algorithm. Compared to the particle swarm optimization algorithm, it improves computational efficiency by 45%. As shown in Fig. 11, the proposed

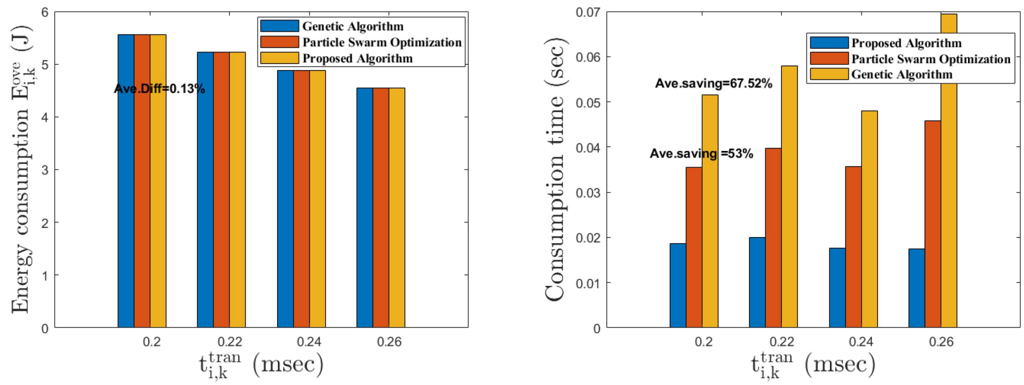

(a) (b)

Fig. 11. Comparison of the proposed algorithm and the baseline algorithms in searching for local optimal solutions and computational efficiency. (a) Comparison between the proposed scheme and the baseline schemes for searching local optimal solutions under different transmission latencies. (b) Comparison of the computational efficiency of the proposed algorithm and the baseline algorithms under different transmission latencies.

algorithm achieves 0.13% difference in accuracy for obtaining local optimal solutions compared to the baseline algorithms. However, it demonstrates superior computational performance, improving computational efficiency by 68% compared to the genetic algorithm and 53% compared to the particle swarm optimization algorithm. In summary, it can be demonstrated that the hierarchical joint optimization proposed algorithm has high accuracy and efficiency.

VI. Conclusion

In this paper, we have proposed a secrecy-oriented resource allocation approach with latency awareness to enhance the immersive experience quality of vehicular users. Through the design of a collaborative rendering architecture, synchronous rendering and real-time aggregation of complex Metaverse scene resources across different computing nodes have been achieved. The objective has been to jointly optimize the offloading decisions of vehicular users, the security threshold of SOP, and transmission latency, aiming to minimize the total rendering latency of the user who has completed last in the vehicular Metaverse system. In response to the non-differentiability and non-convexity of the target problem, a hierarchical joint optimization algorithm has been exploited to decompose the target problem into multiple strictly convex subproblems for the solution. The simulation results have shown that the proposed scheme outperforms benchmark schemes, verifying the feasibility and practicality of the algorithm. In future research, we will further explore the specific applications of Metaverse scenarios in the data perception layer and application layer of internet of vehicle, and formulate a system model that better aligns with practical requirements.

References

[1] Z. Wang, G. Sun, H. Su, H. Yu, B. Lei, and M. Guizani, "Low-latency scheduling approach for dependent tasks in MEC-enabled 5G vehicular networks," *IEEE Internet Things J.*, vol. 11, no. 4, pp. 6278–6289, Feb. 2024.

[2] N. Liu, T. H. Luan, Y. Wang, Y. Liu, and Z. Su, "QoE-oriented cooperative VR rendering and dynamic resource leasing in Metaverse," *IEEE Trans. Mobile Comput.*, vol. 24, no. 10, pp. 10247–10263, Oct. 2025.

[3] C. Xu, Z. Chen, M. Tao, and W. Zhang, "Edge-device collaborative rendering for wireless multi-user interactive virtual reality in metaverse," in *Proc. IEEE Glob. Commun. Conf.*, 2023, pp. 3542–3547.

[4] Y. Li, G. Wu, and J. Tang, "Social-aware edge caching for uav-assisted metaverse systems," in *Proc. IEEE Glob. Commun. Conf.*, 2023, pp. 6898–6903.

[5] M. Cheng, Z. Su, Y. Wu, Q. Xu, M. Dai, and D. Fang, "MEC-enabled cooperative rendering in Metaverse: A coalition formation game approach," in *Proc. IEEE Int. Conf. Commun.*, 2024, pp. 4548–4553.

[6] M. Gao, R. Shen, L. Shi, W. Qi, J. Li, and Y. Li, "Task partitioning and offloading in DNN-task enabled mobile edge computing networks," *IEEE Trans. Mobile Comput.*, vol. 22, no. 4, pp. 2435–2445, Apr. 2023.

[7] X. Wang, J. Ye, and J. C. S. Lui, "Online learning aided decentralized multiuser task offloading for mobile edge computing," *IEEE Trans. Mobile Comput.*, vol. 23, no. 4, pp. 3328–3342, Apr. 2024.

[8] J. Wang, Z. Li, H. Liu, T. Qiu, and H. Luo, "A trust-based computation offloading framework in mobile cloud-edge computing networks," *IEEE Trans. Mobile Comput.*, vol. 24, no. 6, pp. 5370–5385, Jun. 2025.

[9] Z. Wang et al., "Location privacy-aware task offloading in mobile edge computing," *IEEE Trans. Mobile Comput.*, vol. 23, no. 3, pp. 2269–2283, Apr. 2024.

[10] J. Li, G. Sun, L. Duan, and Q. Wu, "Multi-objective optimization for UAV swarm-assisted IoT with virtual antenna arrays," *IEEE Trans. Mobile Comput.*, vol. 23, no. 5, pp. 4890–4907, May 2024.

[11] G. Sun et al., "Generative AI for advanced uav networking," *IEEE Netw.*, vol. 39, no. 4, pp. 244–253, Jul. 2025.

[12] Y. Wu, Y. Song, T. Wang, L. Qian, and T. Q. S. Quek, "Non-orthogonal multiple access assisted federated learning via wireless power transfer: A cost-efficient approach," *IEEE Trans. Commun.*, vol. 70, no. 4, pp. 2853–2869, Apr. 2022.

[13] Y. Li, Y. Wu, M. Dai, B. Lin, W. Jia, and X. Shen, "Hybrid NOMA-FDMA assisted dual computation offloading: A latency minimization approach," *IEEE Trans. Netw. Sci. Eng.*, vol. 9, no. 5, pp. 3345–3360, Sep./Oct. 2022.

[14] M. Dai, Y. Wu, L. Qian, Z. Su, B. Lin, and N. Chen, "UAV-assisted multi-access computation offloading via hybrid NOMA and FDMA in marine networks," *IEEE Trans. Netw. Sci. Eng.*, vol. 10, no. 1, pp. 113–127, Jan./Feb. 2022.

[15] Z. Sun, G. Sun, Y. Liu, J. Wang, and D. Cao, "BARGAIN-MATCH: A game theoretical approach for resource allocation and task offloading in vehicular edge computing networks," *IEEE Trans. Mobile Comput.*, vol. 23, no. 2, pp. 1655–1673, Feb. 2024.

[16] W. Lu et al., "Secure NOMA-based UAV-MEC network towards a flying eavesdropper," *IEEE Trans. Commun.*, vol. 70, no. 5, pp. 3364–3376, May 2022.

[17] X. Gao, Y. Mei, Y. Wang, M. Shi, J. Kang, and K. Yang, "Secrecy energy efficiency maximization in space-air-ground networks with an aerial eavesdropper," *IEEE Trans. Veh. Technol.*, vol. 74, no. 11, pp. 17972–17984, Nov. 2025.

[18] S. Liu et al., "Satisfaction-maximized secure computation offloading in multi-eavesdropper MEC networks," *IEEE Trans. Wireless Commun.*, vol. 21, no. 6, pp. 4227–4241, Jun. 2021.
[19] M. Dai, Z. Su, Q. Xu, Y. Wang, and N. Lu, "A trust-driven contract incentive scheme for mobile crowd-sensing networks," *IEEE Trans. Veh. Technol.*, vol. 71, no. 2, pp. 1794–1806, Feb. 2021.
[20] L. Feng et al., "Resource allocation for metaverse experience optimization: A multi-objective multi-agent evolutionary reinforcement learning approach," *IEEE Trans. Mobile Comput.*, vol. 24, no. 4, pp. 3473–3488, Apr. 2025.
[21] Y. Liu, J. Liu, A. Argyriou, L. Wang, and Z. Xu, "Rendering-aware VR video caching over multi-cell MEC networks," *IEEE Trans. Veh. Technol.*, vol. 70, no. 3, pp. 2728–2742, Apr. 2021.
[22] Y. Jiang et al., "Reliable distributed computing for Metaverse: A hierarchical game-theoretic approach," *IEEE Trans. Veh. Technol.*, vol. 72, no. 1, pp. 1084–1100, Jan. 2023.
[23] H. Du et al., "Attention-aware resource allocation and QoE analysis for Metaverse XURLLC services," *IEEE J. Sel. Areas Commun.*, vol. 41, no. 7, pp. 2158–2175, Jul. 2023.
[24] W. C. Ng, W. Y. B. Lim, Z. Xiong, D. Niyato, X. S. Shen, and C. Miao, "Distributionally robust cost minimized edge semantic intelligence in the sustainable Metaverse," *IEEE Trans. Mobile Comput.*, vol. 23, no. 7, pp. 7910–7926, Jul. 2024.
[25] C. Xu, Z. Chen, M. Tao, and W. Zhang, "Wireless multi-user interactive virtual reality in Metaverse with edge-device collaborative computing," *IEEE Trans. Wireless Commun.*, vol. 24, no. 7, pp. 6135–6150, Jul. 2025.
[26] Z. Long, H. Dong, and A. E. Saddik, "Human-centric resource allocation for the Metaverse with multiaccess edge computing," *IEEE Internet Things J.*, vol. 10, no. 22, pp. 19993–20005, Nov. 2023.
[27] J. Yu, A. Alhilal, T. Zhou, P. Hui, and D. H. K. Tsang, "Attention-based QoE-aware digital twin empowered edge computing for immersive virtual reality," *IEEE Trans. Wireless Commun.*, vol. 23, no. 9, pp. 11276–11290, Sep. 2024.
[28] X. Li, W. Huangfu, X. Xu, J. Huo, and K. Long, "Secure offloading with adversarial multi-agent reinforcement learning against intelligent eavesdroppers in UAV-enabled mobile edge computing," *IEEE Trans. Mobile Comput.*, vol. 23, no. 12, pp. 13914–13928, Dec. 2024.
[29] T. Xiao, C. Chen, Q. Pei, and H. H. Song, "Consortium blockchain-based computation offloading using mobile edge platoon cloud in Internet of Vehicles," *IEEE Trans. Intell. Transp. Syst.*, vol. 23, no. 10, pp. 17769–17783, Oct. 2022.
[30] L. Yin, J. Luo, C. Qiu, C. Wang, and Y. Qiao, "Joint task offloading and resources allocation for hybrid vehicle edge computing systems," *IEEE Trans. Intell. Transp. Syst.*, vol. 25, no. 8, pp. 10355–10368, Aug. 2024.
[31] W. Fan, "Blockchain-secured task offloading and resource allocation for cloud-edge-end cooperative networks," *IEEE Trans. Mobile Comput.*, vol. 23, no. 8, pp. 8092–8110, Aug. 2024.
[32] C. Sun, X. Wu, X. Li, Q. Fan, J. Wen, and V. C. M. Leung, "Cooperative computation offloading for multi-access edge computing in 6G mobile networks via soft actor critic," *IEEE Trans. Netw. Sci. Eng.*, vol. 11, no. 6, pp. 5601–5614, Nov./Dec. 2024.
[33] G. Sun et al., "Joint task offloading and resource allocation in aerial-terrestrial UAV networks with edge and fog computing for post-disaster rescue," *IEEE Trans. Mobile Comput.*, vol. 23, no. 9, pp. 8582–8600, Sep. 2024.
[34] L. Wang and G. Zhang, "Joint service caching, resource allocation and computation offloading in three-tier cooperative mobile edge computing system," *IEEE Trans. Netw. Sci. Eng.*, vol. 10, no. 6, pp. 3343–3353, Nov./Dec. 2023.
[35] R. Xing, Z. Su, and Y. Wang, "Collaborative intrusion detection approach based on blockchain in Internet of Vehicles," *IEEE Internet Things J.*, vol. 12, no. 9, pp. 11965–11976, May 2025.
[36] L. Zhai, Y. Zou, and J. Zhu, "Stackelberg game-based multiple access design for intelligent reflecting surface assisted wireless powered IoT networks," *IEEE Trans. Wireless Commun.*, vol. 22, no. 10, pp. 6883–6897, Oct. 2023.
[37] D. Xu, "Device scheduling and computation offloading in mobile edge computing networks: A novel NOMA scheme," *IEEE Trans. Veh. Technol.*, vol. 73, no. 6, pp. 9071–9076, Jun. 2024.
[38] H. Li, Y. Chen, K. Li, Y. Yang, and J. Huang, "Dynamic energy-efficient computation offloading in NOMA-enabled air-ground integrated edge computing," *IEEE Internet Things J.*, vol. 11, no. 23, pp. 37617–37629, Dec. 2024.
[39] Z. Su, M. Dai, Q. Xu, R. Li, and H. Zhang, "UAV enabled content distribution for internet of connected vehicles in 5G heterogeneous networks," *IEEE Trans. Intell. Transp. Syst.*, vol. 22, no. 8, pp. 5091–5102, Aug. 2021.
[40] J. Wang et al., "Generative AI based secure wireless sensing for ISAC networks," *IEEE Trans. Inf. Forensics Secur.*, vol. 20, pp. 5195–5210, 2025.

Xin Li received the bachelor of Engineering degree in Internet of Things engineering from the Taiyuan University of Science and Technology, Taiyuan, China, in 2023. He is currently working toward the Ph.D. degree with the College of Information and Intelligent Science, Donghua University, Shanghai, China. His research interests include the Internet of Vehicles, wireless communication networks, edge intelligent computing, and the Internet of Things security.

Minghui Dai (Member, IEEE) received the Ph.D. degree from Shanghai University, Shanghai, China, in 2021. He is currently an Assistant Professor with the School of Information and Intelligent Science, Donghua University, Shanghai. His research interests include wireless network architecture and vehicular networks.

Shan Chang (Member, IEEE) received the Ph.D. degree in computer software and theory from Xi'an Jiaotong University, Xi'an, China, in 2012. From 2009 to 2010, she was a Visiting Scholar with the Department of Computer Science and Engineering, Hong Kong University of Science and Technology, Hong Kong. She was also a Visiting Scholar with BBCR Research Lab, University of Waterloo, Waterloo, ON, Canada, from 2010 to 2011. She is currently a Professor with the Department of Information and Intelligent Science, Donghua University, Shanghai, China. Her research interests include security and privacy in mobile networks, and sensor networks. She is a member of IEEE Computer Society, Communication Society, and Vehicular Technology Society.

Liang Zhang received the B.S. degree in computer science and technology from Northeastern University, Shenyang, China, in 2018, and the Ph.D. degree in computer science and technology from Shanghai Jiaotong University, Shanghai, China. She is currently a Lecturer with the School of Information and Intelligent Science, Donghua University, Shanghai. Her research interests include resource scheduling and efficient AI in both cloud and edge computing environments.

Tianshun Wang (Member, IEEE) received the B.Sc. degree in communication engineering from Jilin University, Changchun, China, in 2020, and the Ph.D. degree in computer science from the University of Macau, Macau, China, in 2023. He is currently an Assistant Professor with the School of Communication and Information Engineering, Nanjing University of Posts and Telecommunications, Nanjing, China. His research interests include mobile edge computing, federated learning, and multimodal learning.

Jiaming Pei (Member, IEEE) received the Ph.D. degree from The University of Sydney, Sydney, NSW, Australia. He has authored or coauthored and worked on some papers in the refereed journals and conferences, such as ICLR, IEEE Journal on Selected Areas in Communications, IEEE Transactions on Intelligent Transportation Systems, IEEE Transactions on Network Science and Engineering, IEEE Transactions on Consumer Electronics, and IEEE Transactions on Vehicular Technology. His research interests include the application of data mining and federated learning.

Shahid Mumtaz (Senior Member, IEEE) is currently an IET fellow, IEEE ComSoc Lecturer, and ACM Distinguished Speaker. He has authored four technical books, 12 book chapters, and more than 300 technical articles (more than 200 IEEE Journals/ Transactions, more than 100 conferences, and two IEEE best paper awards) in mobile communications. He was the recipient of the NSFC Researcher Fund for Young Scientist, in 2017 from China and IEEE ComSoC Young Researcher Award, in 2020. He was awarded an Alain Bensoussan Fellowship, in 2012. He is the Founder and EiC of IET Journal of Quantum Communication, Vice Chair of Europe/Africa Region—IEEE ComSoc: Green Communications and Computing society and IEEE standard on P1932.1: Standard for Licensed/Unlicensed Spectrum Interoperability in wireless mobile network.